## Com plex trajectories in chaotic dynam ical tunneling

D.G. Levkov<sup>a1</sup>, A.G. Panin<sup>a,b2</sup>, S.M. Sibiryakov<sup>c;a3</sup>

<sup>a</sup> Institute for Nuclear Research of the Russian Academy of Sciences,
60th October Anniversary prospect 7a, Moscow 117312, Russia.

<sup>b</sup>Moscow Institute of Physics and Technology,
Institutskii per. 9, Dolgoprudny 141700, Moscow Region, Russia.

<sup>c</sup>Theory Group, Physics Department, CERN, CH-1211 Geneva 23, Switzerland.

#### A bstract

We describe sem iclassically the process of chaotic dynam ical tunneling in a quantum mechanical model with two degrees of freedom. A development of the sem iclassical method of complex trajectories is proposed. First, we suggest a systematic numerical technique for obtaining complex tunneling trajectories by the gradual deformation of the classical ones. This provides a natural classication of tunneling solutions. Second, we present a heuristic procedure for sorting out the least suppressed trajectory. Our analysis reveals rich dynamics of the system. At the classical level, there exists an in nite set of unstable solutions forming a fractal structure. This structure is inherited by the complex tunneling paths and plays the central role in the semiclassical study. The process we consider exhibits the phenomenon of optimal tunneling: the suppression exponent of the tunneling probability has a local minimum at a certain energy which is thus (locally) the optimal energy for tunneling. We test the proposed method by comparison of the semiclassical results with the results of the exact quantum computations and not a good agreement. This supports the semiclassical approach to the description of chaotic tunneling.

<sup>1</sup> levkov@ m s2.inrac.ru

<sup>&</sup>lt;sup>2</sup>panin@ms2.inrac.ru

<sup>&</sup>lt;sup>3</sup> Sergey Sibiryakov@cem.ch, sibir@ms2.inrac.ru

### 1 Introduction

An intrinsic feature of quantum physics is the existence of processes which are forbidden at the classical level. The text{book examples of such processes are tunneling and over{ barrier re-ection in one{dimensional quantum mechanics; more involved topics include atom ionization processes [1], chemical reactions [2], false vacuum decay in scalar eld theory [3], etc. Generically, one introduces a certain parameter  $g^2$  (the Planck constant ~ in quantum mechanics, coupling constant in eld theory, etc.) measuring the magnitude of quantum uctuations, and nds that the probabilities P of classically forbidden processes behave exponentially as  $g^2$ ! 0,

P' 
$$g A e^{F=g^2}$$
: (1)

Here F > 0 is the suppression exponent and the explicit dependence of the pre-exponential factor on g is indicated explicitly. In this paper we adopt the term \tunneling" for any process forbidden at the classical level. This includes, in particular, the cases of dynam ical tunneling [2,4], when the exponential suppression of the process is not related to the existence of a potential barrier.

A powerful tool for the study of tunneling at small q<sup>2</sup> is provided by the sem iclassical methods. Exploiting the semiclassical approach, one reduces the problem of computing the tunneling probability to the problem of nding the relevant solution to the classical equations of motion in the complex domain [1, 2, 5], where both the time variable t and dynamical coordinates are taken to be complex. The suppression exponent F is then related to the classical action S calculated along an appropriate contour in the complex time plane. The shape of this contour, as well as the boundary conditions in posed on the solution at 1, are dictated by the quantum numbers of the initial and nalstates. In the simplest cases of under {barrier motion (one-dimensional tunneling, false vacuum decay) the contour runs along the imaginary time axis, and the relevant solution is real along this axis. Such a trajectory may be identied with the \most probable escape path" in the con quration space [6, 3], which gives some understanding of the classically forbidden dynamics. In other cases, however, the passage of the system through the classically forbidden region of the phase space cannot be treated separately from the preceding and following real(time evolution, and the analysis of complex tunneling solutions in the complex time domain is needed. This happens, e.g., in the study of chemical reactions with de nite initial quantum state of reactants [2] or in the investigation of the induced tunneling processes in eld theory [7, 8,

 $<sup>^4</sup>$  In that case one usually introduces the real variable = it, which is called Euclidean time.

9, 10]. The sem iclassical techniques based on genuinely complex classical solutions received the common name of the method of complex trajectories.

It should be pointed out that the application of the above method to a particular system might be highly non (trivial. Major complications are related to the issues of existence and uniqueness of tunneling trajectories, which are basically the complex solutions to a certain boundary value problem. First, it may occur that the boundary value problem at hand does not have any solutions at all (see, e.g., Ref. [11]). Second, there may exist many (sometimes an in nite number of) solutions. Some of them may well be unphysical and should be rejected. The identication of physical solutions relies very much on the particular properties of the system under consideration; presently there are no trustworthy criteria applicable in general (see Refs. [12, 13, 14] for the attempts to not such criteria). Even after the unphysical solutions are eliminated, the problem remains to identify the solution (s) which yield the minimal suppression exponent and therefore correspond to the dominant contribution into the tunneling amplitude. Again, a way to solve this problem depends on the properties of a particular system.

In this paper we make a step towards resolving the disculties of the semiclassical method. We consider the processes which proceed classically at some values of the initial-state quantum numbers, and become exponentially suppressed at other values. The technique presented below enables one to obtain complex trajectories describing tunneling by starting from the real classical solutions and changing gradually the quantum numbers of the initial state. Our procedure has two advantages. First, it is generic and numerically implementable. Second, it provides a natural classication of tunneling trajectories based on the analysis of their classical progenitors. The latter classication suggests a heuristic method for sorting out the least suppressed tunneling path.

As an illustration we apply the above method to the problem of scattering in quantum mechanical model with two degrees of freedom. The process we study is a particular exemple of over-barrier rejection. We calculate the suppression exponent for the rejection probability. As the test of the method we compare the semiclassical results with the \exact" suppression exponent. The latter is extracted from the exact wave function obtained by solving numerically the Schrödinger equation. The results of the two calculations are in good agreement.

The system under consideration has two distinctive features, which are inherent in two wide (intersecting but not necessarily identical) classes of tunneling problems. We believe that our model is a generic representative of both of these classes.

The rst feature is chaoticity. Appearance of chaos is generic for non{linear systems with many degrees of freedom. Quantum properties of chaotic systems have been actively discussed in literature during the last decades. In particular, the topics related to tunneling in the presence of chaos were addressed in Refs. [13, 15, 16, 17, 18, 14, 19].

Let us comment on the relation of chaotic dynamics to the non {perturbative relection process we study. First of all, there is a number of rigorous mathematical denitions of classical chaos, see, e.g. [20]. All of them, however, are applicable to systems whose motion at given energy is connected to a compact region of the phase space. In our case (scattering problem) the motion of the system is unbounded, and it is unclear whether these denitions make any sense at all. For example, a widely used denition of chaos is the requirement that the trajectories with maximal Lyapunov exponent form a set of non {zero measure in the phase space. In common words, this means that a substantial part of classical trajectories are unstable. The analysis of the classical dynamics in our system reveals, however, that the measure of the set of unstable trajectories is vanishingly small. Therefore, one cannot claim formally that chaoticity is present in our model at the classical level: starting from a generic point of the phase space, the system undergoes classical transition (or rejection) governed by a stable trajectory.

The above situation changes as one turns to the complex trajectories describing classically forbidden re ections. The major di erence between the cases of classically allowed and classically forbidden processes is as follows. All real classical trajectories contribute almost equally into the amplitude of the classically allowed rejection (with dierent phase factors eis=gr) implying that the contribution of the vanishingly small set of unstable trajectories is zero. This is no longer valid for the complex trajectories, whose contributions into the am plitude are exponentially di erent (they are, again, proportional to  $e^{iS=g^2}$ , but now the actions S are complex). Therefore, only one distinguished trajectory (or, rather, a small vicinity of this trajectory) contributes into the amplitude. Here lies the root of our claim that the tunneling dynamics of our system is chaotic: the least suppressed complex trajectory describing the process of over{barrier re ection in our system is unstable. Moreover, we nd that the unstable trajectories accumulate in a small vicinity of this distinguished trajectory, so that at any sm all (but still nite) value of the sem iclassical param eter  $q^2$  there exists an in nite number of unstable complex trajectories which contribute almost equally into the re ection am plitude. One expects to encounter most of the features of chaotic tunneling in the case under study, in spite of the absence of chaos at the classical level.

One of the relevant properties we observe is as follows. Consider the set of initial data

giving rise to the classical rejectories. We will see that this set falls into an in nite number of disconnected domains, with unstable trajectories corresponding to the boundaries of these domains. In fact, the above rejection domains develop in nitely nestructures at their boundaries as one increases the resolution of the initial data, so that the set of their boundary points (corresponding to the unstable classical solutions) forms a fractal similar to the Cantor set. The above structures are inherited by the complex tunneling trajectories, whose number is thus in nite. In particular, we will show that the least suppressed tunneling trajectory is a descendant of a certain unstable classical solution lying on the boundary of the above fractal set.

The chaoticity of the process manifests itself in the exact quantum computations as well. We not that the quantum probability of tunneling, instead of being smooth function of energy, exhibits large irregular oscillations. Similar dependence of the tunneling amplitude on the parameters of chaotic systems was reported previously in Refs. [15, 16, 18]. At rest glance, this behavior contradicts to the semiclassical formula (1). One observes, however, that the oscillation period scales like  $g^2$  when  $g^2$ ! O, so that the oscillations become indiscernible in the semiclassical limit. In order to extract the semiclassical suppression exponent, one smears the tunneling probability over several periods. The smeared probability does obey the scaling law (1).

The second feature of our system is as follows. We observe that the process under consideration is classically forbidden, and hence exponentially suppressed, at arbitrary high energies. Our interest in this property is motivated by the studies of similar processes in quantum eld theory. As a matter of fact, the exponential suppression at all energies is generic for the eld theoretical processes involving creation of some classical object (soliton, bubble of new phase or vacuum con guration with dierent topology) in a collision of two highly energetic quantum particles [21, 22, 23, 24, 10]. Moreover, it has been shown recently [10] that the method of complex trajectories predicts the suppression exponent F of the above processes to attain its minimum at a certain \optimal" energy  $E_o$ , above which F stays constant (this behavior of the suppression exponent was conjectured earlier in Refs. [22, 23]). The optimal value F ( $E_o$ ) is determined by the complex (valued classical solutions with particular properties, see Refs [10]; these solutions are called \real{time} instantons".

One m ight question the applicability of the method of complex trajectories for the description of the above phenomenon of optimal tunneling. Indeed, the properties of processes at E  $E_o$  are in many respects dierent from the well{known case of tunneling through}

a potential barrier. In this paper we provide the evidence that the sem iclassical method is applicable for the description of dynamical tunneling independently of how high the energy of the process is, or whether there exists a potential barrier at all.

The model of this paper provides a particular example of quantum mechanical system exhibiting the phenomenon of optimal tunneling. Namely, the suppression exponent F (E) depends on energy E in non-monotonic way, attaining a local minimum at some energy  $E_o$ . We will not that the minimal value of the suppression exponent is indeed given by the method of real-time instantons. At higher energies the function F (E) grows to in nity<sup>5</sup>.

The paper is organized as follows. In Sec. 2 we describe the model under consideration and introduce notations. In Sec. 3 the classical dynamics of the system is analyzed. The sem iclassical study of the classically forbidden rejections is performed in Sec. 4. In Sec. 5 we present the results of the numerical integration of the Schrodinger equation and discuss their comparison with the sem iclassical results. Sec. 6 contains summary and conclusions.

## 2 Setup

We study the evolution of a quantum particle in two-dimensional harmonic waveguide. Namely, we consider the case when the motion of the particle is connect to the vicinity of a certain line  $Y = \frac{1}{g}a(gX)$  by the quadratic potential (X and Y stand for the Cartesian coordinates of the particle). The equipotential contour U (X;Y) = E is shown in Fig.1; the Hamiltonian is

$$H = \frac{P_X^2 + P_Y^2}{2m} + U(X;Y);$$
 (2)

w here

U (X;Y) = 
$$\frac{m!^2}{2}$$
 Y  $\frac{1}{q}$ a (gX) ; a (x) =  $a_0e^{x^2=2}$ : (3)

In the asymptotic regions X! 1, the variables of the model  $\mathbb{Q}$ ) separate, and the motion of the particle becomes trivial: oscillations in the Y-direction are accompanied by the translatory motion along the X-axis. The wriggle around the point X 0 introduces nonlinear coupling between the degrees of freedom; we refer to this part of the conguration

 $<sup>^5</sup>$ This is different from the case of collision{induced tunneling in eld theory, where the suppression exponent stays constant at energies higher than  $E_{\circ}$ . The reason is that in the latter case at  $E > E_{\circ}$  another tunneling mechanism, which is specific for the eld theoretical setup, comes into play. Namely, above the optimal point the energy excess ( $E = E_{\circ}$ ) is released by the emission of a few hard quantum particles, so that the tunneling transition electively occurs at the optimal energy [23, 10].

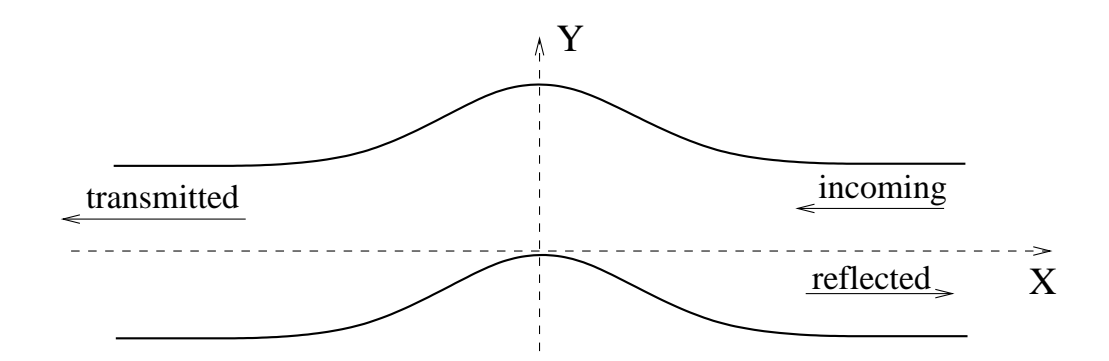


Figure 1: The equipotential contour U(X;Y) = E for the waveguide model (2) and the directions of the incoming, rejected and transmitted uxes of particles.

space as the interaction region. We are not aware of any concrete experimental setup which would be described by the Hamiltonian (2); our model is chosen primarily for simplicity which makes it tractable both semiclassically and by the exact quantum mechanical methods. A system similar to (2) was considered in Ref. [25].

In what follows we use the system of units where

$$\sim = ! = m = 1 :$$
 (4)

The rescaling

$$X = x = q; \qquad P = pq \tag{5}$$

brings the Hamiltonian (2) into the form

$$H = \frac{g^2 (p_x^2 + p_y^2)}{2} + \frac{1}{2g^2} (y - a(x))^2 :$$
 (6)

Equation (6) in plies that the sem iclassical regime in our model occurs for  $g^2$  1. A part from  $g^2$ , the only free parameter of the model (6) is  $a_0$ , which we set

$$a_0 = 0.8$$
: (7)

This choice will be explained in Sec. 3. To avoid confusion, we remark that the rescaled coordinates x, y will be used for the semiclassical analysis of Secs. 3, 4 and App. A, while the original ones (X and Y) are exploited in the quantum computations of Sec. 5 and App. B.

The process we want to investigate is the backward rejection of a particle coming from the right, see Fig. 1. Note that though we will refer to this process as over-barrier rejection,

there is actually no potential barrier in our system: the m in im um of the potential is zero in any transverse section of the waveguide. The incoming quantum state £; N i is completely determined by the total energy E and occupation number N of the Y-oscillator. The quantity of interest is the total re-ection coe cient for this state,

$$P (E;N) = \lim_{t_{f} t_{i}! + 1} \frac{1}{t_{f}} \sum_{f}^{X} hf \dot{f} e^{iH (t_{f} t_{i})} \not{f} : N \dot{i}^{2};$$
 (8)

where jf i stands for the basis of rejected waves ( $P_f > 0$ ) supported in the right asymptotic region, and the proper normalization of the incoming state has been chosen,

$$E; N \not= 0; N = 2 (E E)_{NN} \circ : (9)$$

At some values of the initial(state parameters E, N the rejection process is classically forbidden. [In particular, one expects a particle with high enough translatory momentum  $P_i$  jto pass classically to the other side of the waveguide ending up in the asymptotic region X ! 1 .] In this case the rejection coefficient (8) is expected to obey the semiclassical scaling law (1) at  $g^2 ! 0 .$  Below we concentrate on the calculation of the leading suppression exponent F as function of E, N.

### 3 Classical re ections

Let us start by considering the classical dynam ics of the re-ection process. As we will see in Sec. 4, the analysis of the classical dynam ics is crucial for understanding the classically forbidden re-ections. The results of the present Section will enable us to identify the sets of the initial data (E; N) which correspond to the classically allowed/forbidden re-ections; for brevity we refer to these sets as classically allowed/classically forbidden regions. Note that these are the regions in the initial data plane (E; N); they should not be confused with the classically allowed/forbidden regions in the conguration space. The latter term is not used in this paper.

One notes that the action functional of the model (6) has the form

$$S = S = g^2; (10)$$

w here

$$S = \frac{X^{2} + y^{2}}{2} + \frac{1}{2}(y - a(x))^{2} dt$$
 (11)

does not contain the parameter q at all. Hence, q drops out of the classical equations of m otion. While studying the classical dynamics it is convenient to forget about g and consider the classical system de ned by the rescaled action (11).

In contrast to quantum mechanics, where two quantum numbers E, N determine the initial state completely, the classical evolution is speci ed by four initial conditions. One of these is physically irrelevant. It corresponds to the x coordinate at the initial m om ent  $t = t_i$ , and can be absorbed by the appropriate shift of ti. Note that, still, one should be careful to choose x (t<sub>i</sub>) far from the interaction region; in num erical calculations of this Section the value

$$x(t_i) = 10 (12a)$$

is used. To keep contact with the quantum mechanical formulation we choose the other two initial data to be the total classical energy E and the \classical occupation number" N, which is equal to the initial classical energy of the transverse oscillations. This determ ines the initial velocity of the particle along the waveguide,

$$\underline{\mathbf{x}}(\mathbf{t}_{1}) = \begin{array}{c} \mathbf{p} \\ \overline{2(\mathbf{E} \quad \mathbf{N})} : \end{array}$$
 (12b)

It is worth noting that Eq. (10) im plies the following relation between the classical param eters and their quantum counterparts,

$$E = g^2 E$$
;  $N = g^2 N$ : (13)

The last initial condition is the initial phase of y-oscillator. It parametrizes the initial position and velocity of the particle in the transverse section of the waveguide:

$$y(t_{i}) = P \frac{p}{2N} \cos_{0}; \qquad (14a)$$

$$\underline{y}(t_{i}) = P \frac{p}{2N} \sin_{0}; \qquad (14b)$$

$$\underline{y(t_i)} = \sum_{i=0}^{p} \underline{x_i} \sin x_i \cdot (14b)$$

C learly, a given point of the plane (E; N) belongs to the classically allowed region if classical re ection is possible for some value (s) of  $_0$ . O therwise, we say that this point lies in the classically forbidden region.

At rst glance it may seem that classical re ections are impossible for any values of E, N as there is no potential barrier to prevent the classical particle from going into the left asym ptotic region. Let us make sure that this is not the case by considering the evolution at small E. In this regime the particle moves slow by along the axis x = a(y) of the wavequide

 $<sup>^{6}</sup>$ R ecall that in our units! = 1.

perform ing small and (relatively) rapid oscillations in the orthogonal direction. The frequency !? of the latter oscillations is determined by the curvature of the transverse section of the potential and thus depends on the position x of the particle. It is straightforward to nd that !?  $(x) = \frac{p}{1 + (a^0(x))^2}$ . The energy of the orthogonal oscillations E? divided by their frequency is an adiabatic invariant,

$$\frac{E_?}{!_2(x)} = const = N :$$
 (15)

On the other hand, the conservation of total energy yields,

$$E = \frac{v_k^2}{2} + E_? = \frac{v_k^2}{2} + N^p \frac{1 + (a^0(x))^2}{1 + (a^0(x))^2};$$
 (16)

where  $v_k$  is the projection of the particle velocity onto the axis of the waveguide. Thus, the adiabatic motion in our waveguide is governed by one (dimensional dynamics in the elective potential

$$q - \frac{q}{1 + a_0^2 x^2 e^{-x^2}}$$
U (x) = N 1 + a\_0^2 x^2 e^{-x^2} : (17)

where the explicit expression (3) for the function a(x) has been used. This picture is valid as long as  $\frac{1}{2} = \frac{1}{2}$  1, which is satisfied for E(x) 1.

The potential (17) has the form of two symmetric humps with the maxima  $U_{max}=N$   $\frac{1+a_0^2e^{-1}}{1+a_0^2e^{-1}}$  situated at x=1, see Fig 2. Any particle coming from the right with

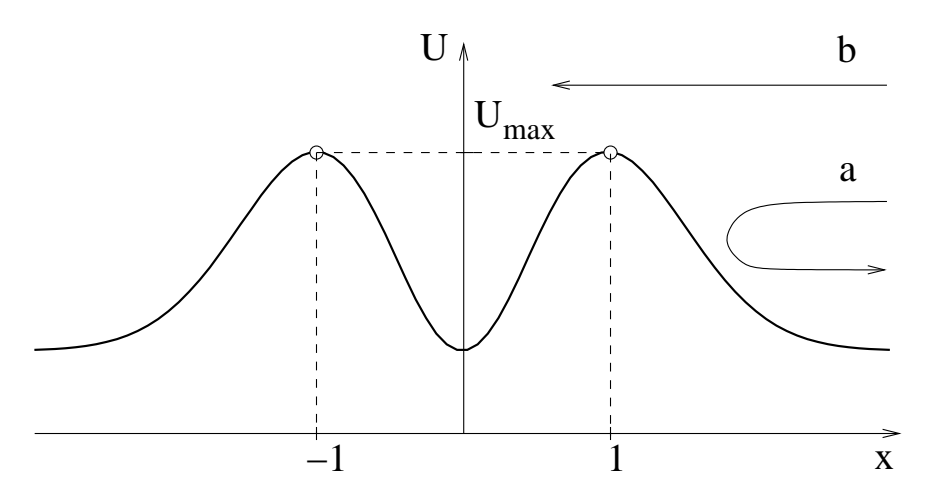


Figure 2: The e ective potential for the motion in the adiabatic regime. The particle is re-ected at E <  $U_{max}$  (case a), and is transmitted through the waveguide at E >  $U_{max}$  (case b).

E <  $U_{m \ ax}$  gets re ected back; so, these values of E , N belong to the classically allowed region. In the opposite case E >  $U_{m \ ax}$  the particle overcom es the e ective potential which m eans that the re ection process is classically forbidden. Thus, the line E = N  $\frac{p}{1+a_0^2e^{-1}}$  is the boundary of the classically allowed region at E;N 1.

When the values of the parameters E, N approach the boundary of the classically allowed region the particle spends more and more time around the tops of the elective barrier U(x). For the values precisely at this boundary there are two unstable solutions x = 1. In the two-dimensional picture these solutions correspond to periodic oscillations around the xed points (x = 1;  $y = a_0e^{-1=2}$ ) on the axis of the waveguide. We will see that such unstable periodic solutions exist beyond the adiabatic approximation and play a key role in the semiclassical analysis. Borrowing the terminology from gauge theories [26, 27] we call them excited sphalerons<sup>7</sup>. The sphaleron living at x = 1 (x = 1) will be referred to as near (far) sphaleron according to its position relative to the right end of the waveguide.

To identify the boundary of the classically allowed region beyond the adiabatic regime one resorts to num ericalm ethods. We scan through the range of initial phases 0 2 at xed E, N and look for the rejected trajectories. If such a trajectory is found at some o, the point (E; N) is identied as belonging to the classically allowed region. Otherwise the point is attributed to the classically forbidden domain. The results of these calculations are presented in Fig.3. The boundaries N<sub>b</sub> (E) of the classically allowed region are obtained for three di erent values of the param eter a<sub>0</sub>. The classical re ections are allowed for the initial data above the boundaries, N >  $N_b$  (E), and forbidden below them, N <  $N_b$  (E). One observes that beyond the adiabatic regime the form of the boundary  $N_b$  (E) depends qualitatively on the value of  $a_0$ . At sm all  $a_0$  it m onotonically increases. At  $a_0$  0.5 a dip in the curve N <sub>b</sub> (E ) develops around E 0:6. As a grows further, this dip becomes lower and m ore pronounced, until it touches the line N = 0 at  $a_0$ 1. At even larger values of a the boundary of the classically allowed region splits into two disconnected parts and a range of energies around E = 0.6 appears, where the classical rejections are allowed even for N = 0.

Heuristically, one may envision that the form of the curve  $N_b(E)$  rejects the behavior of the suppression exponent F(E;N) in the classically forbidden region. Indeed, the suppression exponent is zero above the line  $N=N_b(E)$ . As the value of N gets decreased at inverse exponent is zero above the line  $N=N_b(E)$ . Thus, the deeper the point is in the classically forbidden domain, the larger is F, and vice versa. A coording to this reasoning the dip in the curve  $N_b(E)$  at  $a_0>0.5$  in plies that classically forbidden rejection are least

 $<sup>^{7}</sup>$ The word sphaleron is form ed from the G reek adjective ' os meaning \ready to fall".

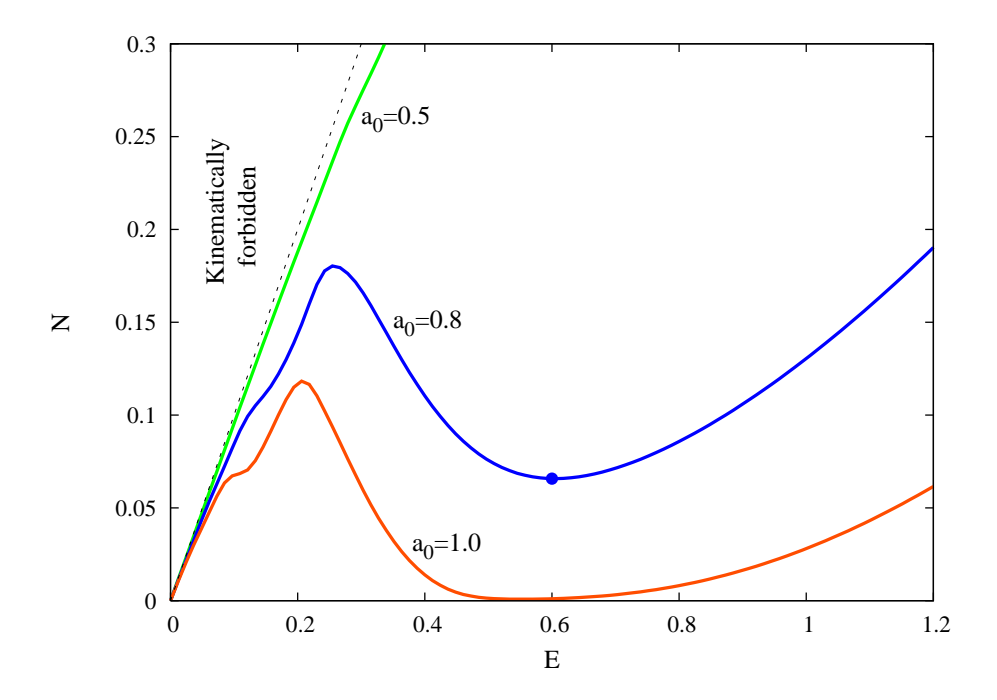


Figure 3: The boundaries  $N_b(E)$  of the classically allowed regions plotted for  $a_0 = 0.5; 0.8; 1.0$ . The classical rejections are forbidden at  $N < N_b(E)$ . The points to the left of the dashed line E = N correspond to the kinematically forbidden initial conditions.

suppressed at energies E 0.6. Moreover, at  $a_0 < 1$  there is a nite range of occupation numbers,  $0 < N < N_b$  (E = 0.6), where the relection process is suppressed at all energies (except for the narrow band  $N < E < N^{\frac{p}{1+a_0^2e^{-1}}}$  corresponding to the adiabatic regime). For these values of N, the suppression exponent F considered as function of E is expected to have a (local) minimum in the vicinity of E = 0.6. One of the purposes of this paper is to test the method of complex trajectories in the regime when the minimum of F (E) exists; so, we concentrate on the case  $a_0 = 0.8$ .

Now, we are in a position to investigate the classical dynam ics of the system (11) in detail. The observations we make below are crucial for the subsequent study of the classically forbidden rejections. One asks the following question. At given E;N belonging to the classically allowed region, there is a non-empty set  $R_{E,N}$  of initial phases o, which give rise to classical rejections. What is the structure of this set? To answer this question, we x the initial conditions (12), (14) at  $t_i=0$  and integrate the equations of motion until

 $<sup>^{8}</sup>$ W e stress that the heuristic argum ents about the behavior of the suppression exponent will be con m ed by the explicit sem iclassical and quantum m echanical calculations in the subsequent sections.

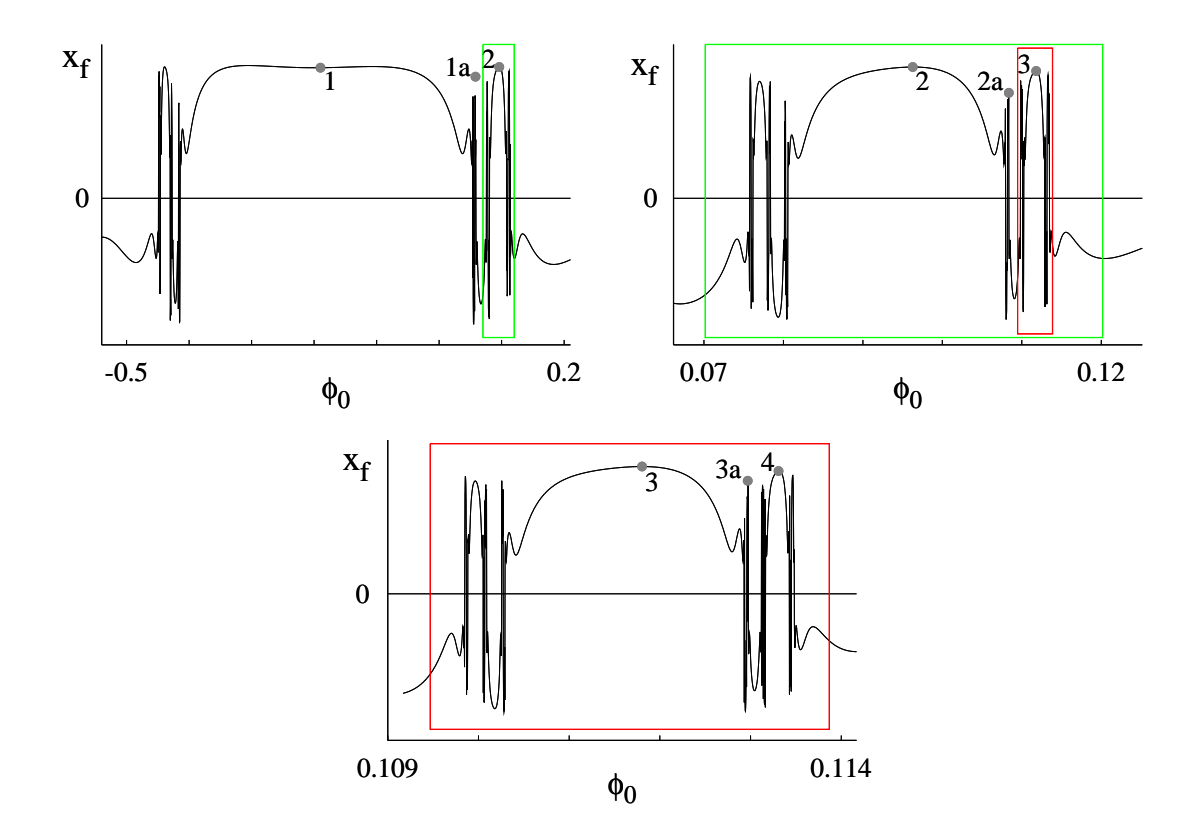


Figure 4: The dependence of the nal particle position on the value of the initial phase  $_0$  for E = 0:6, N = 0:1. From top left to bottom: scaling of the ne structures of the function  $x_f$  ( $_0$ ) reveals self-sim ilar behavior. The corresponding regions in di erent graphs are marked by the boxes of the same color. The trajectories corresponding to the marked points are shown in Fig. 5.

 $t_f = 200$  starting from di erent values of the initial phase  $_0$ . In this way, the dependence of  $x_f = x(t_f)$  on  $_0$  is obtained, see Fig. 4. The negative values of  $x_f$  correspond to the classical transm issions through the waveguide, while  $x_f > 0$  represent rejections. Thus,

$$R_{E,N} = f_{0} \dot{x}_{f}(0) > 0g:$$
 (18)

Figure 4 shows that the set  $R_{E,N}$  is not connected: the intervals of phases corresponding to the rejectories are intermixed with those representing transmissions. Moreover, the scaling of the nestructures of the function  $x_f(0)$  reveals self-similar behavior. One concludes that the set  $R_{E,N}$  consists of an infinite number of disconnected domains forming a fractal structure. Such a complexity is a manifestation of irregular dynamics inherent

in our model; this feature is in sharp contrast to the situation one observes in completely regular systems (see, e.g., the model of Ref. [28] where the analogous set consists of a single interval [27]).

To analyze the nature of irregular dynam ics, we consider the trajectories generated by the initial phases which span various connected intervals R  $_{;E,N}$   $R_{E,N}$ . All the classical trajectories from a given interval of phases display the same qualitative properties; some features change discontinuously, however, as one goes to another interval. Let us characterize each trajectory by its behavior in the interaction region. To start with, one can distinguish a subset of intervals  $R_{j,E,N}$   $R_{E,N}$  corresponding to the trajectories which reach the far sphaleron, perform several oscillations there, and go out of the interaction region back to x + 1. We call this subset the main sequence". The x-th-dependence for the rst four trajectories from the main sequence is plotted in Fig. 5a, while the corresponding values of the initial phase are marked in Fig. 4a by numbers (1 to 4). Let us make the important

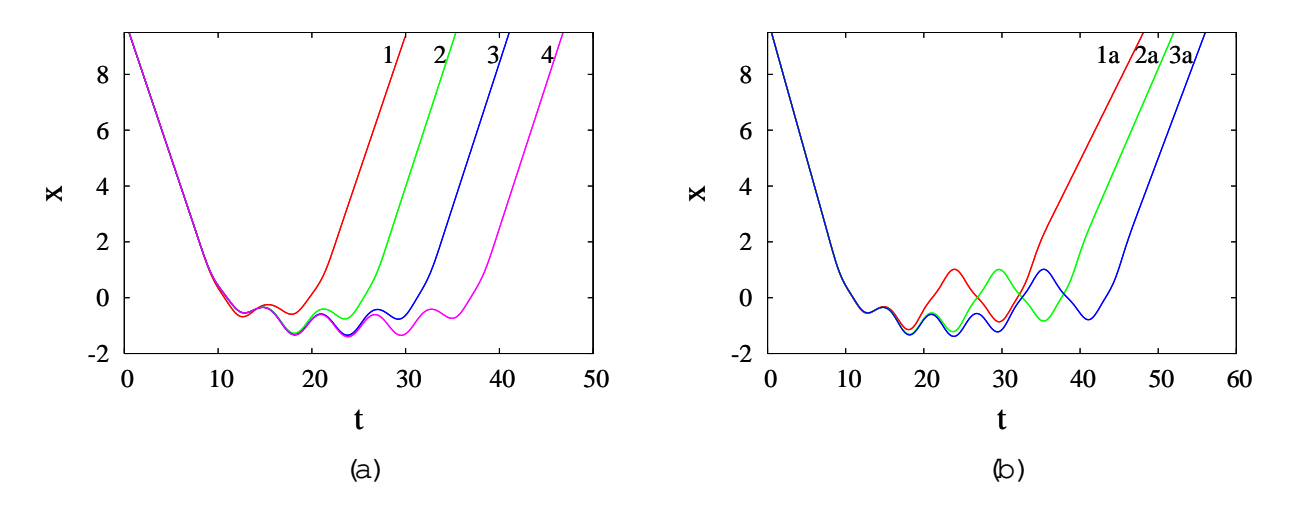


Figure 5: The main (a) and secondary (b) sequences of trajectories for E = 0.6, N = 0.1. The trajectories correspond to initial phases with the same marks as in Fig.4.

observation: all the plotted solutions leave the far sphaleron with approximately the same oscillatory phase. In fact, we have found that this is true for any rejected trajectory. Here lies the root of the disconnectedness of  $R_{E,N}$ : one cannot transform one rejected trajectory into another with a different number of oscillations at the far sphaleron by continuously changing the initial phase. For a solution from the main sequence the index j is equal to the number of oscillations at x.

The trajectories corresponding to the intervals of  $R_{E,iN}$  other than those from the main

sequence display more involved behavior. A fler oscillating at the far sphaleron they move to the near sphaleron, oscillate an integer number of periods on top of it, return to the far sphaleron, oscillate there once again, etc. As an example we present several trajectories from the next-to-the-main sequence (with only one return to the far sphaleron) in Fig. 5b. We observed that the motion back and forth between the sphalerons can be arbitrarily complicated giving rise to the aforementioned fractal structure of R  $_{\rm E,N}$ .

For the sem iclassical analysis of the next Section it is important to know what happens with the classical rejected solution when the initial phase  $_0$  approaches the end-point  $_{\rm end}$  of an interval R  $_{\rm E,N}$   $_{\rm RE,N}$  . Figure 4 implies that at the ends of the interval the corresponding trajectory gets stuck in the interaction region. More precisely, one observes that as the value of  $_0$  approaches  $_{\rm end}$ , the classical solution spends more and more time at  $_{\rm end}$  1 before going away to in nity (see Fig.6), so that the initial datum  $_0$  =  $_{\rm end}$  gives rise

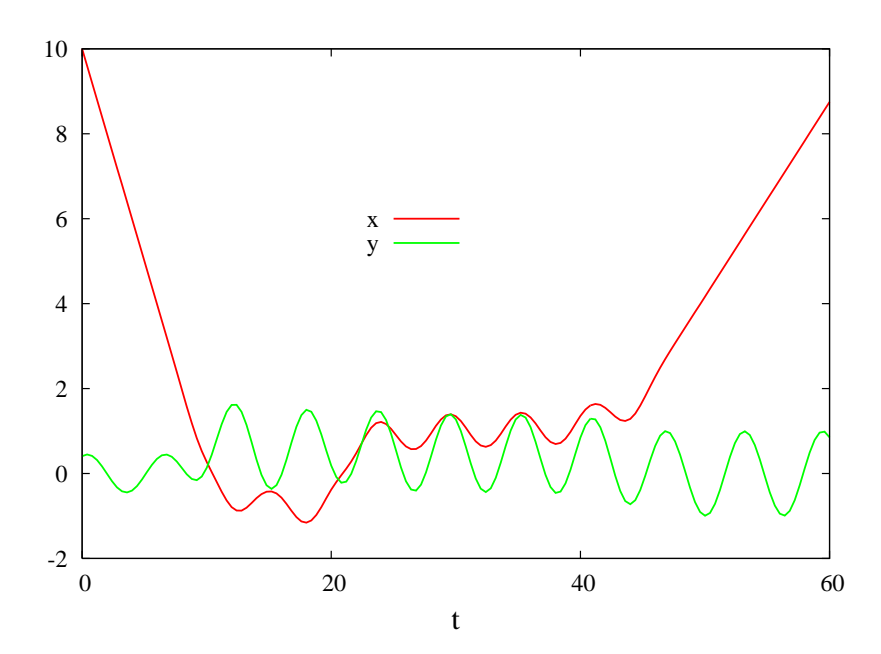


Figure 6: The classical trajectory with the value of the initial phase  $_0 = 0.414$  close to the end{point,  $_0$   $_{\rm end}$   $10^3$ , of the rst interval of the main sequence; E = 0.6, N = 0.1. Before leaving the interaction region the trajectory gets stuck at the near sphaleron for a long time.

to a trajectory which is neither rejected, nor transmitted, but ends up at the near sphaleron. Such a trajectory is unstable: there exist arbitrarily small perturbations which push it out of the interaction region to either end of the wavequide. As the number of intervals (and

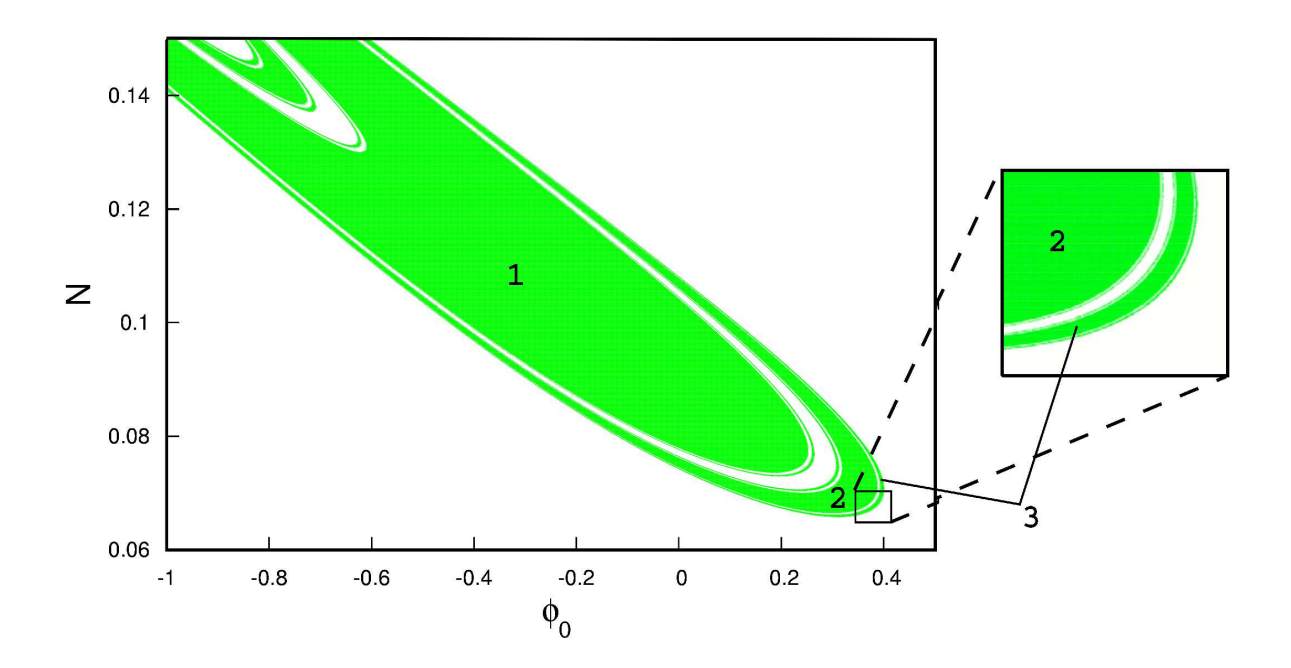


Figure 7: The set R  $_{\rm E}$  of initial data leading to re-ections at E = 0.6 (painted in green). The inset shows the ne structure near the boundary of R  $_{\rm E}$ . Three rst domains of the main sequence are marked by numbers.

hence of their end-points) constituting R  $_{\rm E,N}$  is in nite, the number of the above unstable trajectories is in nite, too. The measure of the set of end {points is, however, zero. This is the consequence of the unboundedness of motion. Indeed, almost every trajectory leaves the interaction region in a nite period of time and goes to in nity, where the motion is stable. Because of the above property we cannot legitimately pretend that our model is really chaotic at the classical level. However, as we will see in the next Section, the above unstable solutions give rise to the tunneling trajectories; thus, the classically forbidden rejector process of the next Section provides a particular example of chaotic tunneling.

M ore insight into the classical dynam ics is gained by extending the previous analysis to include the variation of two initial conditions,  $_0$  and N , at xed energy E . One is again interested in the structure of the set R  $_{\rm E}$  of initial data ( $_0$ ;N) which correspond to classical rejections. This set is shown in Fig. 7 (E = 0:6). As before, it consists of an in nite number of disconnected domains R  $_{\rm E}$ . Each of these domains is characterized by the way in which

the corresponding trajectories travelback and forth between the sphalerons. The domains of the main sequence with j=1;2;3 are clearly visible in Fig. 7 along with the secondary ones which accompany them. Figure 7 enables one to understand what happens with the classical rejectories when the occupation number N approaches the boundary of the classically allowed region from above, N !  $N_b(E)$ ; this corresponds to moving to the lower boundary of the set  $R_E$ ,

$$N_b(E) = \inf_{(0,N)2R_E} N$$
:

One notices that no matter how close N is to this boundary, the line N = constalways has intersections with some domains from the main sequence. In other words, the boundary of the classically allowed region is the accumulation point of the main sequence of domains. On the other hand, as N tends to N<sub>b</sub>(E), the intersection of the line N = const with certain domains of R<sub>E</sub> disappears. This means disappearance of certain types of trajectories at N! N<sub>b</sub>(E). Concentrating on the main sequence, one observes that the remaining trajectories are those with large indices j. As the latter are equal to the number of oscillations at the far sphaleron, one concludes that the closer the point (E;N) is to the boundary of the classically allowed region, the longer the corresponding trajectories get stuck at the far sphaleron.

We conclude this section with remarks on the implications of the above classical picture for the semiclassical description of tunneling. It will be shown in Sec. 4 that each isolated domain of the set R  $_{\rm E}$  continues into a branch of tunneling trajectories. Thus, the number of tunneling solutions at given E , N < N  $_{\rm b}$  (E ) is in nite; each of these solutions is associated with a certain domain R  $_{\rm iE}$ . In particular, the fractal structure of R  $_{\rm E}$  is inherited by the collection of tunneling paths. The above property is very different from that of the models with completely regular classical dynamics [27] where the tunneling solution is unique. On the other hand, an in nite number of tunneling trajectories seems to be generically inherent in chaotic systems [18]. A coording to the general rules, the suppression exponent F in Eq. (1) is equal to the lower bound of the suppressions calculated on all the tunneling solutions,

$$F (E;N) = \inf F (E;N); \tag{19}$$

where the index marks the solutions. At rst glance it is not clear how the lower bound (19) can be found: one is unable to compute the suppression exponents of an in nite set of

 $<sup>^9</sup>$ This property should not be confused with the property described in the previous paragraph, where it was pointed out that the trajectories get stuck at the near sphaleron when the initial data approach the boundary of a single domain R  $_{i,E}$  of R  $_{E}$ .

trajectories. Two observations which greatly simplify the problem are as follows. First, it will be shown below that the nearer the domain R  $_{;E}$  is to the boundary of the classically allowed region, the smaller is the suppression exponent of the tunneling solution associated with it. Second, the domains of the main sequence accumulate near the boundary of the classically allowed region. This implies that the suppression exponents  $F_j$  of the tunneling trajectories from the main sequence with the index j. Moreover, for any tunneling path there exist tunneling solutions from the main sequence with the same E, N and smaller value of the suppression exponent. Thus, in order to calculate the lower bound (19) it is su cient to consider the trajectories from the main sequence, compute their suppression exponents  $F_j$ , and take the lim it,

$$F (E;N) = \lim_{j! = 1} F_j(E;N)$$
: (20)

This tactics is implemented in the next section.

## 4 Sem iclassical study

We now formulate the boundary value problem for the tunneling trajectories. The probability (8) of over-barrier rejection is described by the complexied solution to the classical equations of motion

$$\frac{S}{x(t)} = \frac{S}{y(t)} = 0 \tag{21a}$$

obeying the following boundary conditions,

$$\frac{\underline{x}^2}{2} + N = E$$
;  $\frac{\underline{y}^2}{2} + \frac{\underline{y}^2}{2} = N$ ; at t! 1; (21b)

Im x; Im y! 0; at 
$$t! + 1$$
: (21c)

Here E, N stand for the (rescaled, see Eqs. (13)) energy and initial occupation number. <sup>11</sup> The initial conditions (21b) att! 1 can be cast into the form (12b), (14), where the initial phase  $_0$  is now allowed to take complex values. Similarly,  $x(t_i)$  is also complex, in general. The boundary conditions (21b), (21c) have clear physical interpretation. Equations (21b) x the quantum numbers E, N of the initial quantum state. Due to the uncertainty principle this

 $<sup>^{10}\,\</sup>mathrm{T}\,\mathrm{hese}$  are the ones originated from the main sequence R  $_{\mathrm{i;E}}$  of domains.

<sup>&</sup>lt;sup>11</sup>N ote that the boundary value problem (21) is invariant with respect to time translations: if x(t), y(t) is a solution to Eqs. (21), then x(t+), y(t+) is also solution for any 2 R. We x this ambiguity by requiring Rex( $t_i$ ) = 10 (cf. Eq. (12a)).

m akes the two conjugate coordinates,  $_0$  and  $x(t_i)$ , m axim ally indeterm in ate. A coordingly, in the sem iclassical picture they become complex (valued. On the other hand, the quantum numbers of the nal states are not xed, and Eqs. (21c) imply that the particle comes out in a classical state with real coordinates and momenta.

Note that, generically, the tunneling solution is de ned along a certain contour in the complex time plane. In our case, however, the contour is trivial: it runs along the real time-axis.

It is useful to parametrize the imaginary parts of  $x(t_i)$  and 0 as follows,

$$2 \operatorname{Im} x (t_i) = \underline{x}(t_i) T ; \qquad (22)$$

$$2 \text{ Im }_{0} = T$$
 ; (23)

where T and are real parameters. Then the suppression exponent of a given complex trajectory is

$$F = 2 \text{ Im } S \qquad E T \qquad N \qquad ; \tag{24}$$

where the two last terms result from the non {trivial initial state of the process, while

$$S = \frac{1}{2} dt \quad xx \quad yy \quad (y \quad a(x^2))$$
 (25)

is the classical action integrated by parts. The subscript  $\,$  is introduced to rem ind that there m ay exist several tunneling solutions with given E , N .

We do not present the derivation of the above boundary value problem. The logic is completely analogous to that of Refs. [28, 27, 29, 30], and an interested reader is referred to these papers. The eld theory analog of the problem (21) was rst introduced in Ref. [7].

It is important to remark that the problem (21) does not guarantee per se that its solutions describe re ections. To ensure that this is the case, one supplements Eqs. (21) with the condition

Rex! +1 at t! +1: 
$$(26)$$

Below we nd solutions which satisfy this requirement by using the {regularization method of Refs. [27].

Let us explain the physical m eaning of the initial-state parameters T, . One can prove the relations (see, e.g., Refs. [27, 30])

$$T = \frac{\theta}{\theta E} F (E; N); = \frac{\theta}{\theta N} F (E; N);$$
 (27)

which imply that T and are the derivatives of the suppression exponent with respect to energy and initial oscillator excitation number. One notices that T, can be used instead of E, N to parametrize the tunneling paths. Then, the solutions with T=0 correspond to the extrem a of the suppression exponent with respect to energy. These solutions are called \real{time} instantons", they can be found directly using the method of Ref. [10]. Calculating the value of the functional (24) on them, one obtains the extremal (notably, minimal) values of the suppression exponent at N= const. The method of real{time} instantons is important in eld theory [10], where it enables one to calculate the minimal suppression of the collision { induced tunneling. One of the purposes of this paper is to check the above method by the explicit comparison with the exact quantum mechanical results. A coordingly, we pay specic attention to the region around the minimum of the suppression exponent F (E).

We solve the boundary value problem (21) numerically with the deformation procedure. Namely, the solution with energy E + E and oscillator excitation number N + N is found by the iterative Newton {Raphson method [31] starting from the solution at E, N, which serves as the zeroth {order approximation. In this way, an entire branch of tunneling trajectories can be obtained starting from a single solution and walking in small steps in E, N. The details of our numerical technique can be found in Refs. [28], see Refs. [8, 9] for the applications in eld theory.

The only non-trivial task of the above approach is to nd the input for the rst deformation. The idea we put forward in this paper is to start the procedure from the classically allowed region and arrive at the tunneling solutions by changing the values of E, N in small steps. One begins with the observation that the real classical trajectories satisfy 2 Eqs. (21). Naively, one takes a trajectory with E, N from the classically allowed region, and decreases the value of N with the hope to get the correct tunneling solution at N < N  $_{\rm b}$  (E ). However, serious obstacles arise on the way. First, the classical solution is not unique at given E, N; the degeneracy is parametrized by the initial phase  $_0$  2 R  $_{\rm E, iN}$  . This makes the numerical im plem entation of the deform ation procedure problem atic. Second, suppose one takes the initial data (N; 0) belonging to some connected domain R:  $R_{E}$  and decreases N . It was observed in Sec. 3 that, as the value of N approaches the boundary N =  $N_b$ ; (E) of R ; from above, the re ected classical solution spends more and more time in the interaction region. At  $N = N_b$ ; (E) it gets stuck at x 1 forever, merging at this point with the classical solutions, which represent the transm issions of the particle through the waveguide at N < N<sub>b</sub>; (E). Here lies the worst obstruction: the transmitted classical trajectories

<sup>&</sup>lt;sup>12</sup>Their suppression is obviously zero.

obviously solve the boundary value problem (21), so that the deform ation procedure which starts from the classically allowed region will produce them at N < N  $_{\rm b}$ ; , instead of the correct complex rejected solutions. One concludes that the condition (26) should be somehow incorporated explicitly into the boundary value problem .

A method which automatically xes the asymptotic (26) of the solution is proposed in Refs. [27,29]. It is called {regularization. Here we brie y describe this method concentrating on its application to the problem at hand. A more detailed description of the technique can be found in Refs. [27,29]. One replaces the action of the system in Eqs. (21), (24) with the modi ed action

$$S [x] = S [x] + i T_{int} [x]$$
: (28)

Here is small and positive, while the functional  $T_{\rm int}$  measures the time the particle spends in the interaction region. The simplest choice is

$$T_{int} = dtf(x(t);y(t));$$
 (29)

where the function f is real and positive at x; y 2 R, and is localized in the interaction region. Otherwise the choice of f is arbitrary: the nal result is recovered in the limit ! + 0 and does not depend on the particular form of this function. We use

$$f = (1 x)(x 1);$$
 (30)

w here

$$^{\sim}(x) = \frac{1}{1 + e^{2x - x^3}}$$
 (31)

is the smeared {function. Note that f peaks at the near sphaleron; this choice will be explained shortly.

One notices two important changes that the substitution (28) brings into the boundary value problem (21). First, the degeneracy of the classical solutions is removed at  $\in$  0. Indeed, any unperturbed classical trajectory extrem izes the original action functional S [x], so that at xed E, N and = 0 there exists a valley of extrem a parametrized by 0. The functional  $T_{\rm int}$  [x], however, discriminates among all these extrema and lifts the valley. Correspondingly, at small > 0 the extrema of the regularized action S [x] are close to the classical rejected solutions with  $\theta T_{\rm int} = \theta_0 = 0$  (see Refs. [27] for the detailed discussion). From the physical viewpoint this can be understood as follows. In the {regularized case the suppression, Eq. (24), of the trajectories in the classically allowed region is not precisely zero because of the complex term i  $T_{\rm int}$  in Eq. (28). The suppression is minimized on the

real classical trajectories corresponding to the m in ima of  $T_{\rm int}$ ; therefore, the solutions to Eqs. (21), (28), which by construction correspond to the least suppressed rejections, are close to the above classical trajectories.

In practice, one starts with the function  $T_{\rm int}(_0)$  representing the values of  $T_{\rm int}$  on the classical trajectories with xed E , N and = 0, nds the extrem a of this function, and uses the corresponding trajectories as the zeroth (order approximation to the solutions of Eqs. (21), (28) with small, but non-zero .

The second useful property of the {regularization comes about as one tries to decrease the value of the initial oscillator excitation number, and cross the boundary  $N = N_{\rm b}$ ; (E) of a given classically allowed domain. One discovers that at 60 each relected trajectory at  $N > N_{\rm b}$ ; (E) is smoothly connected with the complex relected solution at  $N < N_{\rm b}$ ; (E). The reason, again, lies in the additional suppression caused by the term i  $T_{\rm int}$  in the action. Although the relected trajectories get only slightly perturbed at small, the solutions ending up in the interaction region at t! +1 change drastically. Indeed, the functional  $T_{\rm int}[k]$  diverges on the latter trajectories giving rise to the initial excitation region are excluded from the set of solutions to the boundary value problem (21), (28). Now, the solutions to Eqs. (21), (28) cannot change their asymptotic (26): starting from the classical relected solution and decreasing the value of the initial excitation number N in small steps, one leaves the classically allowed region and obtains the correct complex relected trajectories.

Let us brie y comment on the choice of the contour in the complex time plane which carries the tunneling solutions. Obviously, the classical trajectories, which are the starting point of our deform ation procedure, run along the real time axis. Generically, while moving into the classically forbidden region, one may need to deform the time contour in order to avoid the singularities of the solution, see Refs. [27]. In the actual calculations of this paper we did not encounter such a necessity. The time contour was always kept coincident with the real axis.

An example of a regularized tunneling solution deep inside the classically forbidden region (E = 0.6, N = 0) is shown in Fig. 8b. The depicted solution descends from the classical rejectory with E = 0.6, N = 0.1,  $_0$  = 0.366 (see Fig. 8a), which (locally) m in in izes the function  $T_{\rm int}(_0)$ ; the regularization = 10  $^6$  was switched on and N was gradually decreased by small steps. Note that the solution in Fig. 8b is genuinely complex and satis es the requirement (26).

The solutions to the original boundary value problem are recovered in the  $\lim it ! + 0$ ;

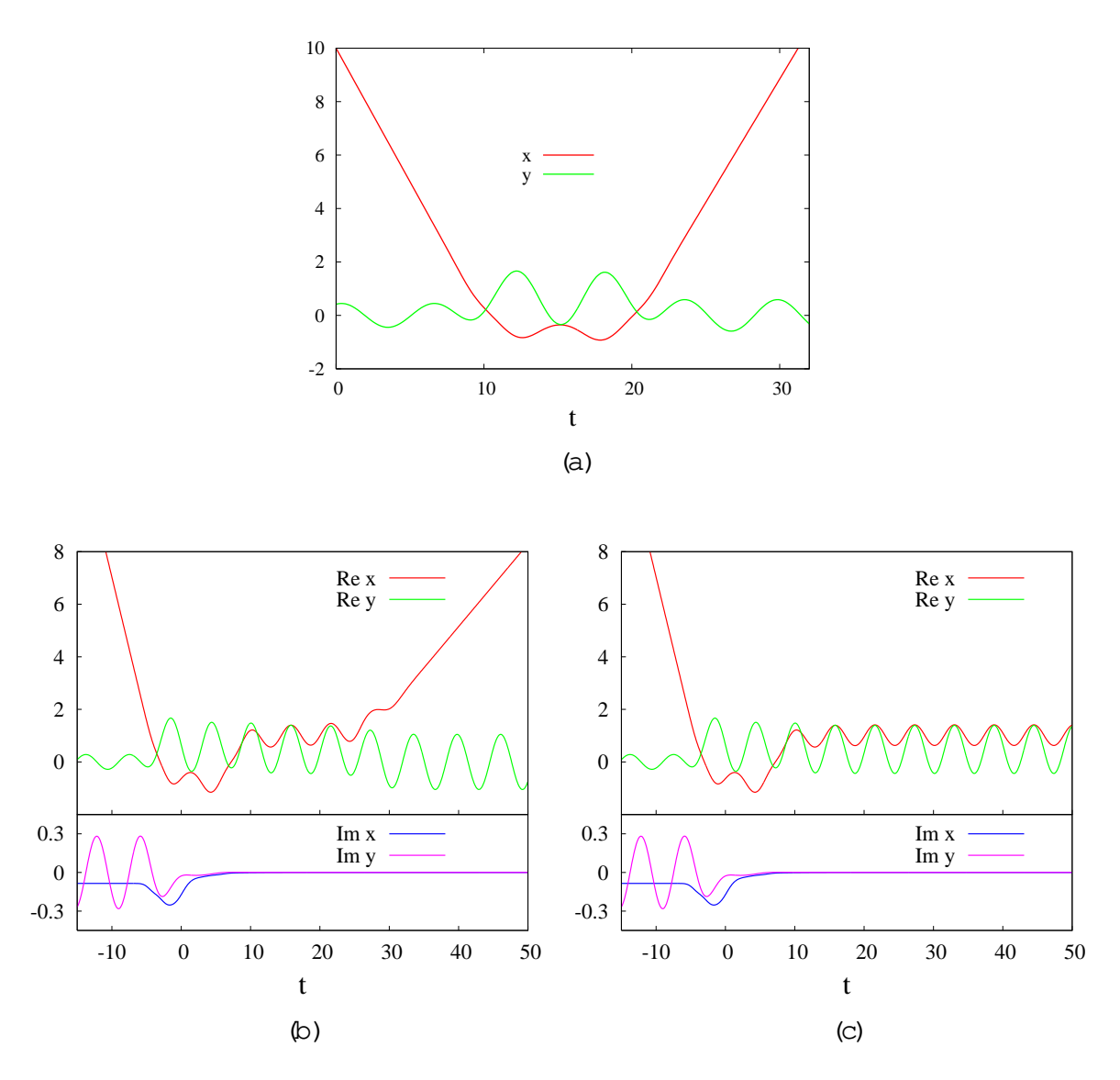


Figure 8: (a) The re-ected classical trajectory from the rst domain of the main sequence, corresponding to the minimum of  $T_{\rm int}(_0)$  (E = 0:6; N = 0:1;  $_0$  = 0:366). (b) The regularized tunneling solution (E = 0:6, N = 0, = 10  $^6$ ) descended from the above classical trajectory. (c) The limit ! 0 of the tunneling solution.

the suppression exponents of the unperturbed trajectories are

$$F (E;N) = \lim_{! \to 0} F_{!} (E;N) :$$
 (32)

P ractically, the rem oval of the regularization is carried out by taking  $\,\,$  to be small enough,  $\,\,^<$  10  $^6$ . At these  $\,$ , the values of the suppression exponents F  $_{;}$  stabilize at the level of accuracy O (10  $^5)$  which is su cient for our purposes.

As one tries to take the lim it ! + 0 of the tunneling trajectory itself, a surprise comes about. Namely, as gets decreased, the regularized tunneling trajectories deep inside the classically forbidden region stay longer and longer at nite x, so that the trajectories with = 0 do not escape to in nity, but end up on an unstable solution  $\{$  the near sphaleron  $\{$  living at x = 0. An example of unperturbed tunneling trajectory (E = 0:6, N = 0, = 0) is shown in Fig. 8c.] Strictly speaking, the solutions at = 0 do not describe rejection, but rather creation of the unstable state, the sphaleron. Nevertheless, their suppression exponents are relevant for tunneling as the latter state decays<sup>13</sup> into the asymptotic region = 0 x = 0 without exponential suppression. Similar behavior of tunneling trajectories was reported previously in Refs. [27].

We remark that all unregularized tunneling trajectories in the model under consideration tend to the unstable sphaleron solution at  $t \,! \, + 1$ , and thus turn out to be unstable them – selves. Straightforward numerical methods are inappropriate for noting such trajectories [28], while {regularization provides a universal method for treating such instabilities  $^4$ .

Let us now discuss the structure of tunneling solutions. Following the above strategy, one starts with the classical rejected solutions. It is straightforward to see that the function  $T_{\rm int}(\ _0)$  has at least one extremum in every connected interval  $R_{\ _{\rm E},N}$  in the set of rejection phases  $R_{\ _{\rm E},N}$ . Indeed, the classical rejectories with  $_{\ _{\rm O}}$  2  $R_{\ _{\rm E},N}$  spend in the interaction region and smoothly depend on the initial data, producing the smooth function  $T_{\rm int}(\ _0)$ . On the other hand, the classical trajectories spend more and more time at the near sphaleron as  $_{\ _{\rm O}}$  approaches the end-points of  $R_{\ _{\rm E},N}$  (see Sec. 3). Thus,  $T_{\rm int}(\ _0)$  tends to in nity at the end points of this interval, necessarily attaining a minimum somewhere in between  $^{15}$ . Note that the special form of the functional  $T_{\rm int}$  (function fine  $T_{\rm E}$  (29) peaks at  $T_{\rm O}$  1) has been chosen in accordance with the tendency of classical trajectories to get stuck at the near sphaleron.] Thus, starting from each interval  $T_{\rm E}$  is the section of the set  $T_{\rm E}$  by the line  $T_{\rm E}$  2 const, the domains of  $T_{\rm E}$  2 may correspond to two disconnected intervals of  $T_{\rm E}$  3, see  $T_{\rm E}$ 4. When  $T_{\rm E}$ 5 are a correspond to two disconnected intervals of  $T_{\rm E}$ 6, see  $T_{\rm E}$ 7. When  $T_{\rm E}$ 8 decreased, these intervals merge. Below we assume that the starting classical solution of the type has been taken at small enough

<sup>&</sup>lt;sup>13</sup>C lassically, the particle sits at the sphaleron for an in nite period of time. However, quantum uctuations lead to the decay of this state with the carachteristic time of order logg.

 $<sup>^{14}\</sup>mathrm{An}$  alternative would be to change the boundary conditions (21c), see App.A.

 $<sup>^{15}</sup>$  In general, there m ight be several extrem a of  $T_{int}$  inside each connected interval  $R_{iE,N}$ , and one should consider solutions corresponding to each of these extrem a. In our case the m in im um is unique.

N, such that the domain R  $_{;E}$  gives rise to a single interval of phases  $^{16}$  R  $_{;E,N}$ . Then, the fractal structure of R  $_{E}$  is inherited by the complex tunneling paths: the distinct branches of complex trajectories are in one {to {one correspondence with the connected domains of the set R  $_{E}$ .

Now, we can give a heuristic justi cation of the claim made in the end of Sec. 3: the nearer the domain R  $_{;E}$  R<sub>E</sub> lies to the boundary of the classically forbidden region, the less suppressed is the corresponding tunneling trajectory. Let us consider two branches of solutions stemming from the domains 1 and 2 in Fig. 7. The line N = 0.07 intersects with the domain 2, so that the point E = 0.6, N = 0.07 belongs to the classically allowed region, and the suppression of the solution 2 vanishes in the limit ! 0.0 n the other hand, the line N = 0.07 does not cross the domain 1. Thus, at E = 0.6, N = 0.07 the corresponding solution to Eqs. (21), (28) is genuinely complex and has non-zero suppression even at ! 0. Suppose that one decreases N and enters the classically forbidden region. At some point the solution of the type 2 also becomes classically forbidden. It is clear that at least for some range of N, its suppression remains weaker than that of the solution 1. This suggests, though does not guarantee, the same hierarchy of suppressions inside the entire classically forbidden region. Below, we check the conjectured hierarchy explicitly.

Let us discuss in detail the case N=0 (no transverse oscillations in the initial state) corresponding to the extrem e values of parameters inside the forbidden region; all the qualitative features are the same for other values of N as well. Our strategy is to not the lim it (20) of the main sequence of suppressions  $F_j$ , and check that this lim it represents the lower bound of the suppression exponents of all the tunneling solutions.

Figure 9 shows several rst representatives of the main sequence of tunneling paths at E=0.5, N=0,  $=10^6$ . Similar to their classical progenitors, the branches of tunneling trajectories may be classified according to the number of oscillations they perform at the far sphaleron. On the contrary, the number of oscillations at the near sphaleron is not an invariant of the branch: as discussed above, it grows as the regularization parameter—gets decreased, so that the tunneling trajectories get stuck at the near sphaleron at =0. A nother important observation about the plots in Fig. 9 is that the imaginary parts of the solutions

 $<sup>^{16}</sup>$ O ne legitim ately asks what happens if the starting classical solution is taken at large enough N , where two di erent intervals of phases correspond to one and the same domain of R  $_{\rm E}$  . C learly, in this case the above deform ation procedure will produce two di erent solutions to Eqs. (21), (28). We have observed, however, that as the value of N gets decreased below the point where the two intervals merge, the corresponding solutions become identical.

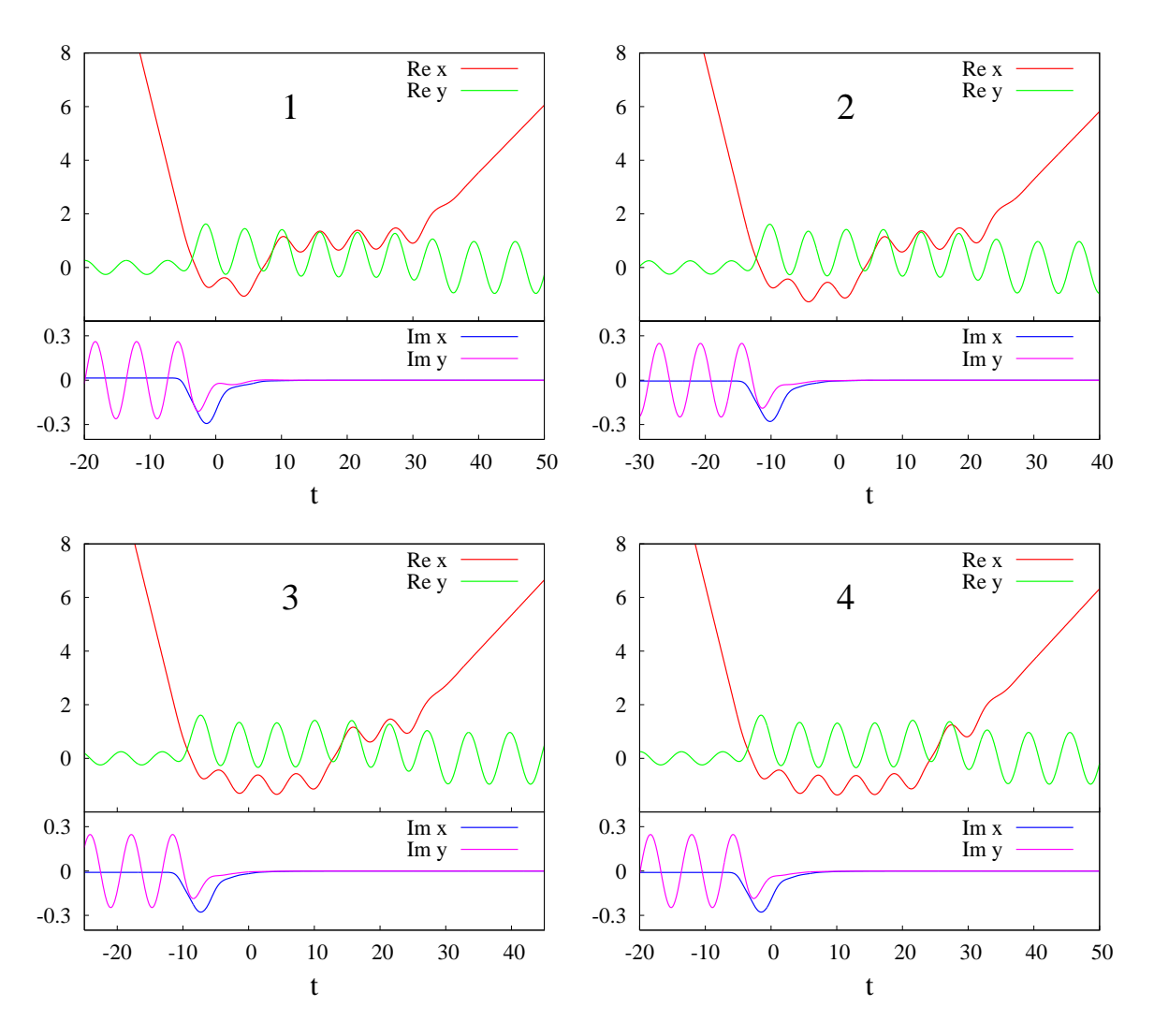


Figure 9: Four tunneling solutions from the main sequence; E = 0.5, N = 0,  $= 10^{6}$ .

are sizeable only in the beginning of the evolution. They fallo rapidly during the oscillations at the far sphaleron and become small at late times. This qualitative feature holds for the trajectories at other energies as well<sup>17</sup>. Thus, the suppression exponents of the trajectories are saturated during the rst few oscillations at the far sphaleron, and depend weakly on the subsequent evolution. In addition, the trajectories from the main sequence almost coincide in the beginning of the process. This implies fast convergence of the suppression exponents  $F_j$  to the limiting value F according to the formula (20).

 $<sup>^{17}</sup>$ On the contrary, the sm allness of Im x at t! 1 observed in Fig. 9 is peculiar to the trajectories at E = 0.5. It implies that the corresponding values of T are sm all, see Eq. (22), so the plotted trajectories are close to the real-time instantons.

ј Е	0.1	0.3	0.5	0.7	0.9
1	0.3188	0.1625	0.1098	0.1398	0.2259
2	0.2586	0.1380	0.0991	0.1341	0.2221
3	0.2373	0.1340	0.0979	0.1336	0.2219
4	0.2307	0.1333	0.0978	0.1336	0.2219
5	0.2285	0.1331	0.0978	0.1336	0.2219
1	0.2272	0.1331	0.0978	0.1336	0.2219

Table 1: The suppression exponents of the complex trajectories from the main sequence at N=0. The rows represent the indices j of the trajectories, while the columns correspond to the values of energy E. The last row refers to the limiting solution.

The above convergence is demonstrated in Table 1, where the suppression exponents  $F_j(E)$  are presented for several values of energy E at N=0. As expected from the heuristic argument, the value of  $F_j$  decreases as j gets larger. The limiting values F (E) are also included into Table 1. They can be obtained by extrapolating the dependences of the suppression exponents  $F_j$  on j, which are well tted by the formula

$$F_i = F + ae^{bj}$$
;

where a, b are real positive coe cients. A better way, which is exploited in this paper, is to not the lim it j! +1 of the tunneling solution itself, and then calculate the lim iting value of the suppression exponent using Eq. (24). The lim iting solution performs an in nite number of oscillations on the far sphaleron; it can be obtained numerically by the method described in App. A. The lim iting solution at E = 0.5, N = 0 is shown in Fig. 10.

So far we have considered only the tunneling trajectories from the main sequence and demonstrated that Eq. (20) reproduces the lower bound of their suppressions. We have checked that the limiting value F (E) is lower than the suppression exponents of other tunneling trajectories as well. As an illustration, consider the tunneling trajectories shown in Fig. 11. The differences between their suppression exponents and that of the limiting solution are plotted in Fig. 12. The limiting solution is evidently the least suppressed one.

Let us discuss the physical interpretation of the obtained results. The form of the limiting solution implies that the rejection process in our model proceeds in two stages. First, the far sphaleron state gets created. This stage is exponentially suppressed due to the essential modication of the particle state needed for the sphaleron creation. Second, the sphaleron

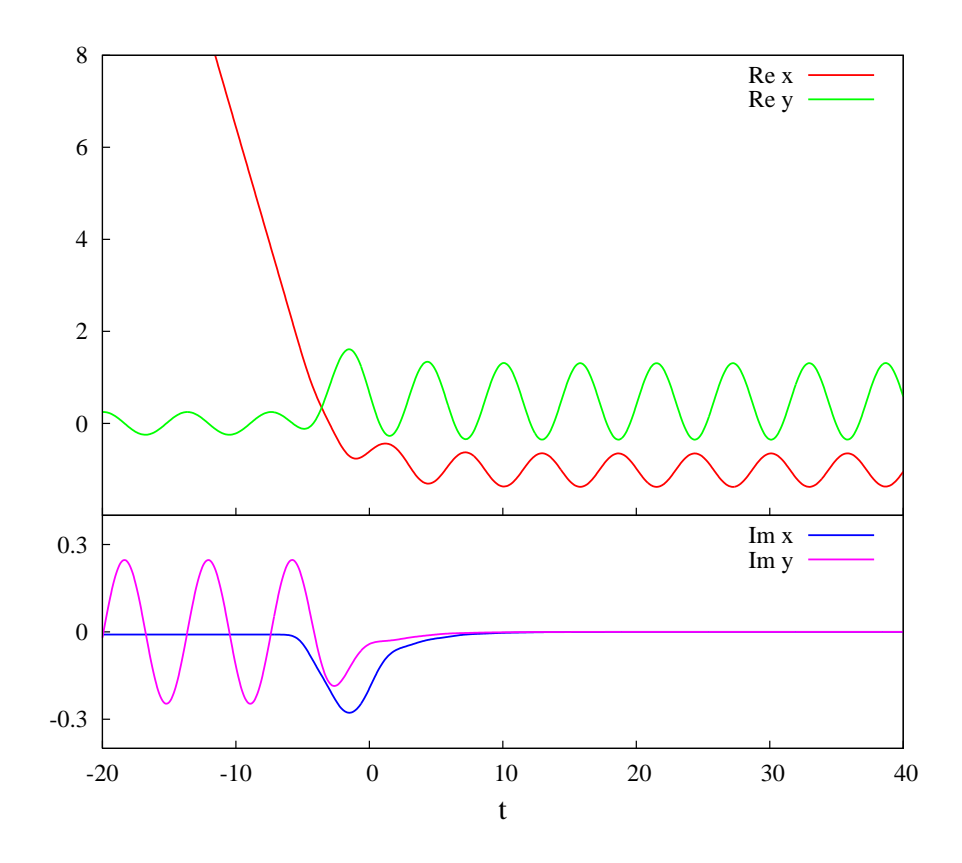


Figure 10: The  $\lim$  it of the main sequence of tunneling trajectories: the solution which gets stuck at the far sphaleron; E = 0.5, N = 0.

state decays into the asym ptotic region  $x \,! \, + 1$  with probability of order 1. This two-stage process is a manifestation of the phenomenon of \tunneling on top of the barrier" [27]; the phenomenon is generic for the inclusive tunneling processes, see Refs. [9, 10] for the eld theoretical examples.

Rem arkably, though we came to the limiting solution considering the accumulation point of an in nite number of complicated tunneling paths, the solution itself is unique and very simple. All the chaotic features of motion, like going back and forth between the sphalerons, are related to the second stage of the rejection process: the decay of the far sphaleron. As the second stage is unsuppressed, one might conclude that, after all, the chaotic motions are irrelevant for the calculation of the main suppression exponent. Note, however, that one is not be able to guess from the beginning, which tunneling solution corresponds to the smallest suppression; therefore, the systematic analysis of the chaotic motions is essential. Besides, the sub-dominant contributions of the chaotic trajectories might be important for

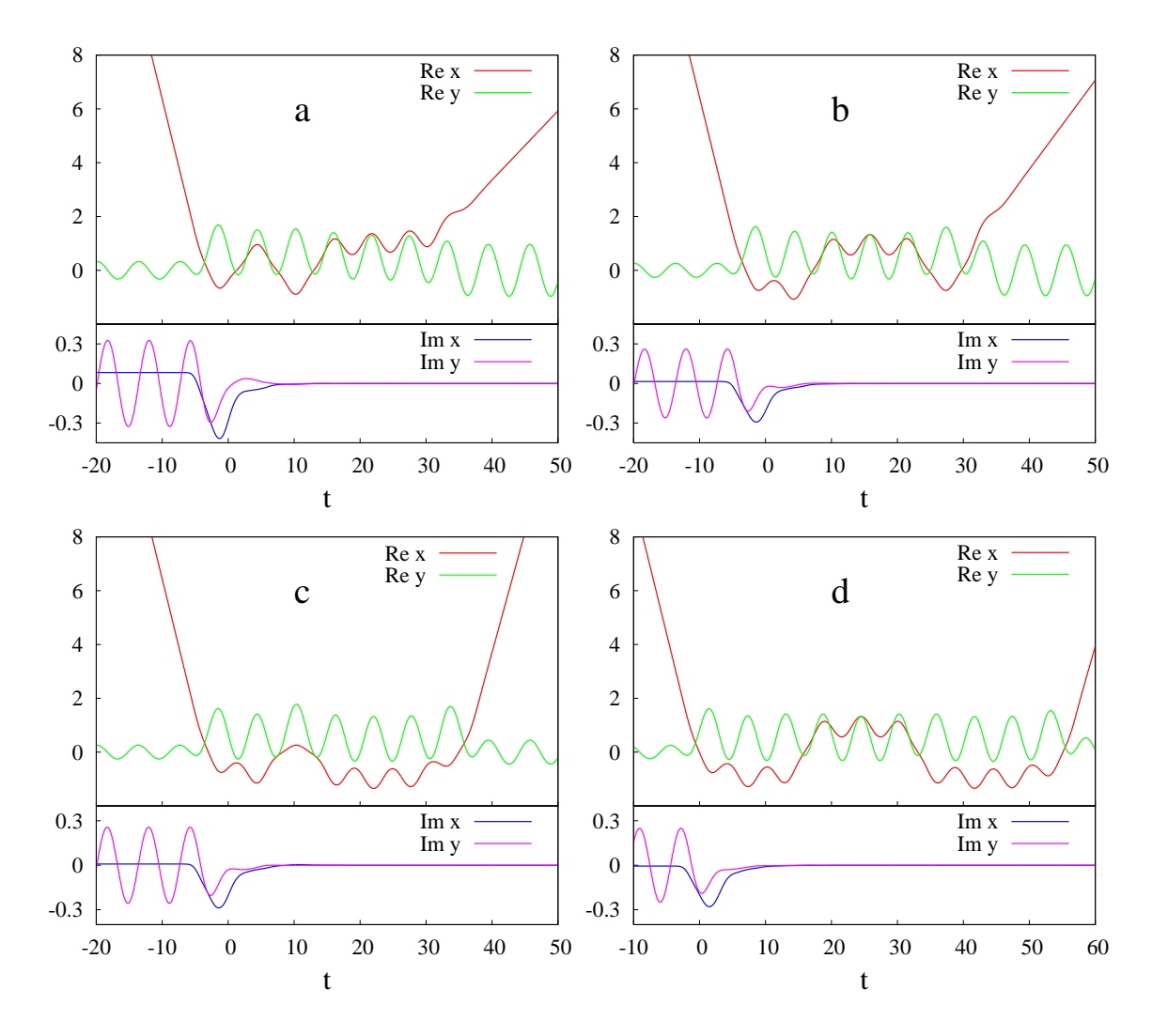


Figure 11: The examples of secondary tunneling trajectories; E = 0.5, N = 0,  $= 10^6$ .

the analysis of the process at nite values of the sem iclassical parameter g [13, 14].

The nal sem iclassical results for the dependence of the suppression exponent F on energy E for N = 0; 0:02; 0:04 are presented in Fig. 13. Note that the suppression exponent is non-monotonic function of energy with the minimum near  $E = 0.5.^{18}$  W e remind that the minima of F (E) correspond to the particularly interesting solutions, real(time instantons.

<sup>&</sup>lt;sup>18</sup> In the range E < 0.1, which is not shown in Fig. 13, the suppression attains the local maximum and goes down to zero as E decreases toward the boundary of the classically allowed region.

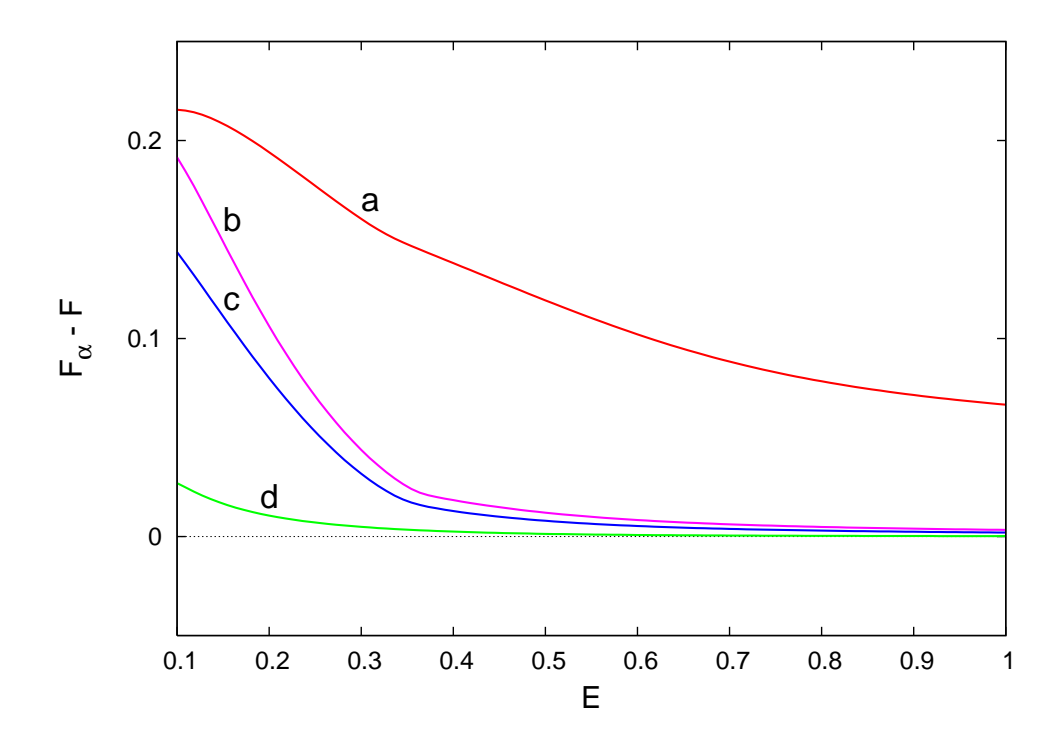


Figure 12: The di erence between the suppression exponents of the secondary trajectories of the types shown in Fig. 11 and that of the  $\lim i \text{ting solution}$ ; N = 0.

# 5 Exact quantum com putations

In this Section we extract the suppression exponent F from the exact re ection probability (8). One begins by solving numerically the Schrödinger equation

$$H j i = E j i$$
: (33)

It is convenient to work in the original variables X, Y,  $P_X$ ,  $P_Y$ , see Eq. (5), in order to bring the kinetic term of the H am iltonian into the canonical form. One rewrites Eqs. (2), (3) as

$$H = \frac{P_X^2 + P_Y^2}{2} + \frac{1}{2} (Y - \alpha (X))^2;$$
 (34)

w here

$$a(X) = \frac{1}{q}a(gX)$$
: (35)

Basically, our numerical technique follows the lines of Refs. [28, 32]. One works in the asymptotic basis formed by a direct product of the translatory coordinate eigenfunctions

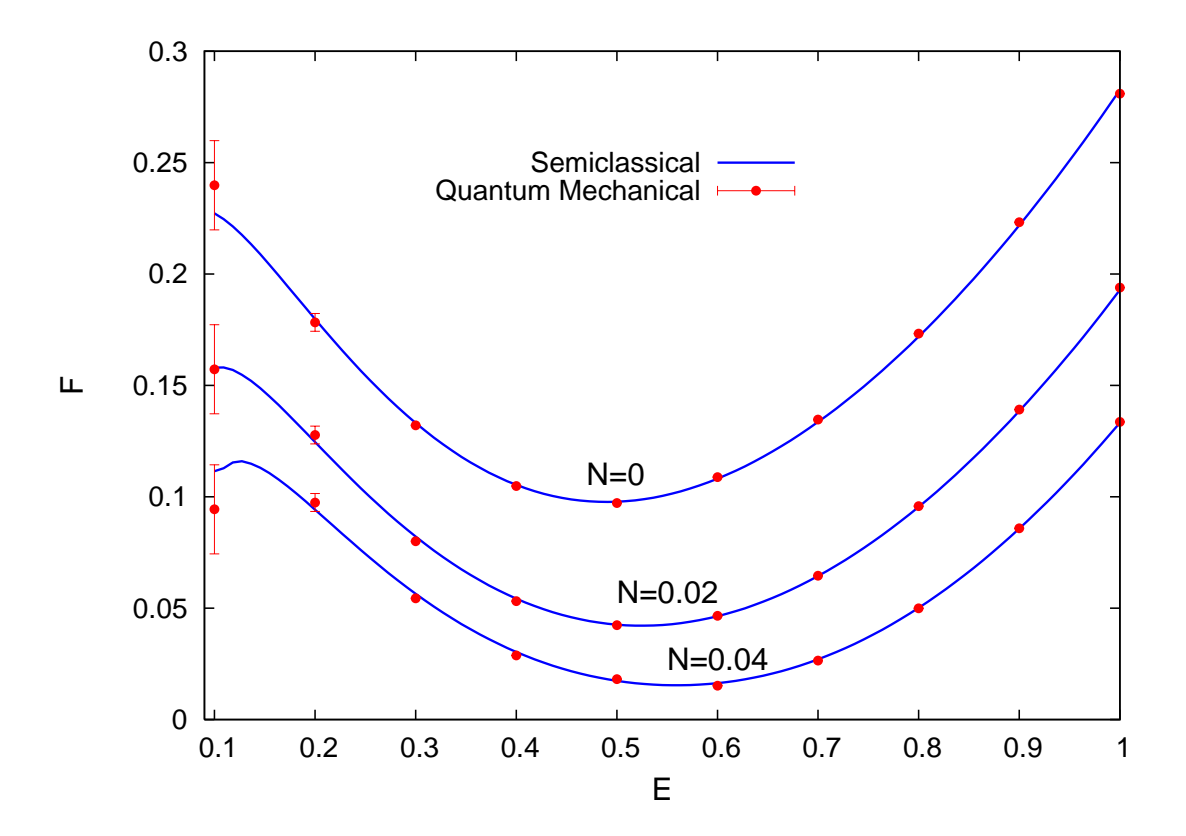


Figure 13: The sem iclassical (lines) versus quantum mechanical (points) results for the suppression exponent F (E) at three dierent values of N. The errors of the quantum mechanical computations are smaller than the point size for E 03.

X i and eigenfunctions in i of the y {oscillator with the xed frequency ! = 1,

$$_{n}$$
 (X ) = hX; nj i:

The stationary Schrodinger equation (33) reads,

$$\frac{d^2}{dX^2} _n (X) = \sum_{n^0}^{X} A_{nn^0} (X) _{n^0} (X); \qquad (36)$$

w here

is an in nite three{diagonalmatrix.

In the asymptotic regions X ! 1 , a(X) ! 0 the interaction terms become negligibly small, and the solution takes the form,

$$_{n}$$
 (X)!  $r_{n} e^{iP_{n}X} + t_{n} e^{iP_{n}X}$ ; (37)

w here

$$P_n = {p \over 2E (2n+1)}$$
 (38)

stands for the asym ptotic translatory m om entum of the n-th m ode. The boundary conditions for the stationary wave function  $_n$  (X ) are constructed in the standard way. The particle com es from the right, X  $\,!\,+1$ , in the N  $\,$  {th oscillator state; hence, we  $\,$ x

$$t_{n}^{+} = {}_{n,N} :$$
 (39)

On the other hand, only the outgoing wave should remain at X! 1,

$$r_n = 0 : (40)$$

Note that while the low (lying modes are oscillatory at the asymptotic, the ones with n > 1=2 grow (decay) exponentially, see Eq. (88). Physically, the latter correspond to the kinetically inaccessible region, where the energy of the transverse oscillations exceeds E. We x the boundary conditions for them by killing the parts growing exponentially toward in nities. One notes that after the proper continuation of Eq. (38),

$$P_n = i \frac{p}{(2n+1)} \frac{}{2E}; \quad n > E \quad 1=2;$$
 (41)

the aforem entioned conditions coincide with Eqs. (39), (40).

Equations (36), (39), (40) constitute the boundary value problem to be solved numerically. After the stationary wave function  $_{\rm n}$  (X ) is found, one calculates the probability current

$$J = \operatorname{Im} \prod_{n=1}^{X} (X) \frac{d}{dX} n(X);$$
 (42)

and hence the re ection probability

$$P = \frac{jJ^{(out)}j}{jJ^{(in)}j} = \sum_{n < E} \frac{P_n}{P_N} jr_n^+ j^2;$$
 (43)

where the currents  $J^{(in)}$  and  $J^{(out)}$  are computed with the incoming and outgoing parts of the wave function at X + 1, respectively.

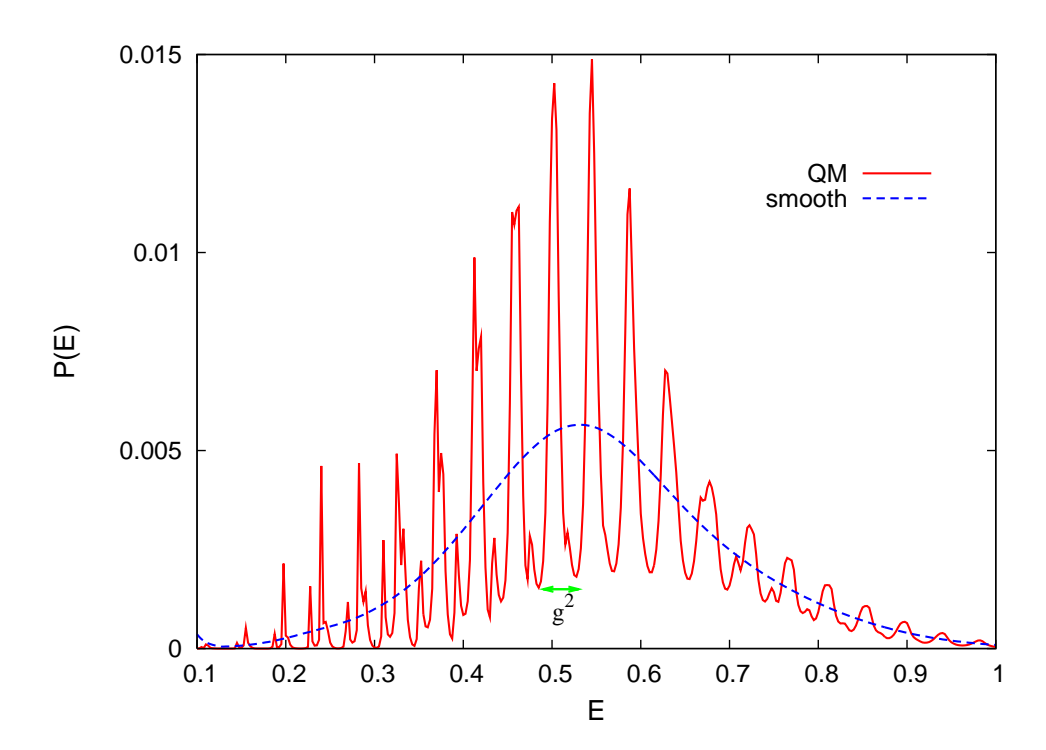


Figure 14: The function P (E) plotted for N = 0, g = 0.2. The dashed curve represents the sm oothened result, Eq. (45).

The details of the numerical formulation of the problem (36), (39), (40) are presented in App.B. Let us discuss the results. The typical dependence of the rejection probability P on energy  $E = g^2E$  is shown in Fig. 14, solid line (the values of the other parameters are N  $g^2N = 0$ , g = 0.2). The striking feature is that the graph is modulated by sharp oscillations. At its glance, this picture is incompatible with the results of the semiclassical analysis, where we obtained, at least in the leading order, that the tunneling probability, P / e  $^{F(E)=g^2}$ , is a smooth function of energy. We are going to demonstrate the opposite: the quantum mechanical results reconcile nicely with the semiclassical ones.

By computing the re-ection probability at di-erent g, one notices the following important properties. First, the period of oscillations scales like  $_{\rm E}$  /  $\rm g^2$ . So, in the sem iclassical limit g! 0 the oscillations become more and more frequent. Second, one considers  $\rm F_g$  =  $\rm g^2$  log P and asks whether the amplitude of oscillations of this quantity goes to zero in the limit g! 0. We certainly observed that it drops down as g decreases though we were unable to

gure out<sup>19</sup> whether it indeed vanishes at g! 0. The properties mentioned above suggest the interpretation of the oscillations as the result of the quantum interference between the contributions of various tunneling trajectories found in Sec. 4. Suppose for simplicity that there are only two such trajectories. Let us denote their complex actions by  $S_1$  (E) and  $S_2$  (E) (we om it the dependence on N). Then, the total rejection amplitude reads,

$$r A_1 e^{iS_1 (E)=g^2} + A_2 e^{iS_2 (E)=g^2}$$
:

For the sake of argum ent we suppress the index n and disregard the initial (state contributions into the exponents. In the above form ula  $A_1$  and  $A_2$  stand for the pre-exponential factors of the partial processes. For the re-ection probability one writes,

$$P / \dot{j}r\dot{j} = ^{2m S_1 (E) = g^2} + ^{2m S_2 (E) + S_2 (E) + S_2 (E) + S_2 (E) = g^2} + ^{2m S_2 (E) + S_2 (E) + S_2 (E) + S_2 (E) = g^2} + ^{2m S_2 (E) + S_2 (E) + S_2 (E) = g^2} + ^{2m S_2 (E) + S_2 (E) + S_2 (E) = g^2} + ^{2m S_2 (E) + S_2 (E) + S_2 (E) = g^2} + ^{2m S_2 (E) + S_2 (E) + S_2 (E) = g^2} + ^{2m S_2 (E) + S_2 (E) + S_2 (E) = g^2} + ^{2m S_2 (E) + S_2 (E) + S_2 (E) = g^2} + ^{2m S_2 (E) + S_2 (E) + S_2 (E) = g^2} + ^{2m S_2 (E) + S_2 (E) + S_2 (E) = g^2} + ^{2m S_2 (E) + S_2 (E) + S_2 (E) = g^2} + ^{2m S_2 (E) + S_2 (E) + S_2 (E) = g^2} + ^{2m S_2 (E) + S_2 (E) + S_2 (E) = g^2} + ^{2m S_2 (E) + S_2 (E) + S_2 (E) = g^2} + ^{2m S_2 (E) + S_2 (E) + S_2 (E) = g^2} + ^{2m S_2 (E) + S_2 (E) + S_2 (E) = g^2} + ^{2m S_2 (E) + S_2 (E) + S_2 (E) = g^2} + ^{2m S_2 (E) + S_2 (E) + S_2 (E) = g^2} + ^{2m S_2 (E) + S_2 (E) + S_2 (E) = g^2} + ^{2m S_2 (E) + S_2 (E) + S_2 (E) = g^2} + ^{2m S_2 (E) + S_2 (E) + S_2 (E) + S_2 (E) = g^2} + ^{2m S_2 (E) + S_2 (E) + S_2 (E) + S_2 (E) = g^2} + ^{2m S_2 (E) + S_2 (E) + S_2 (E) + S_2 (E) = g^2} + ^{2m S_2 (E) + S_2 (E) + S_2 (E) + S_2 (E) = g^2} + ^{2m S_2 (E) + S_2 (E) + S_2 (E) + S_2 (E) = g^2} + ^{2m S_2 (E) + S_2 ($$

A long with the term's corresponding to the probabilities of the partial processes, one gets the interference term, which results in oscillations with period  $_{\rm E}$  of order  ${\rm g}^2$ . O focurse, if one of the solutions, say, the rst one, is dominant, Im  ${\rm S}_1<{\rm Im}\,{\rm S}_2$ , the relative contributions of the two last terms in Eq. (44) vanish exponentially fast at  ${\rm g}$ ! 0. In our case the situation is more subtle, however. As the sem iclassical analysis reveals, in the model under consideration there exists an in nite number of tunneling paths, which pile up near the dominant limiting solution. So, at each nite value of g there are solutions which satisfy Im  $({\rm S}_2-{\rm S}_1)$ .  ${\rm g}^2$  (the index \1" still marks the dominant solution here). Thus, the sum (44) always contains an in nite number of oscillating terms producing a complicated interference pattern; it is not clear whether the oscillations disappear at small g.

W hat saves the day is the aforem entioned scaling of the oscillation period. Indeed,  $_{\rm E}$  vanishes at g! 0 implying that the oscillations become indiscernible in the semiclassical limit. One obtains a quantity which is well-behaved in this limit by averaging the reection probability over several periods of oscillations. To be more precise, we consider the smoothened probability

$$P^{(s)}(E;N) = dE^{0}D(E E^{0})P(E^{0};N);$$
(45)

where D is the bell-shaped function,

D (E) = 
$$\frac{e^{E^2=2}}{P}$$
; Z dE D (E) = 1:

 $<sup>^{19}\</sup>text{T}$  his is due to the limitations of the numerical approach: one cannot obtain solutions to the Schrödinger equation at arbitrarily small g, see App.B.

If  $= g^2$ , where is a xed number, the smoothening (45) does not spoil the value of the dominant suppression exponent. Indeed, for the rst term in Eq. (44) one writes,

Z
$$P^{(s;dom)} / dE^{0} / A_{1} / e^{F_{1}(E^{0}) = g^{2}} D (E^{0} E) / A_{1} / e^{F_{1}^{0}(E) = g^{2}}; (46)$$

where  $^{20}$   $F_1=2\text{Im }S_1$ ,  $F_1^{\,0}=dF_1=dE$ , and we made use of the Taylor series expansion in the second equality. It is clear that only the pre-exponential factor is a ected by the integration (45), while the exponent  $F_1$  (E) is left intact. On the other hand, at large enough values of the coe cient—the formula (45) represents averaging overmany oscillatory periods, which kills all the oscillating contributions. Indeed, consider the typical interference term,

$$P^{(osc)} / C \times e^{F_0 \times E} = g^2 \cos S \times E = g^2$$
 (E); (47)

where  $F_0 = \text{Im } (S_1 + S_2)$ ,  $S = \text{Re}(S_1 - S_2)$ ,  $C = 2 / A_1 A_2$ ;  $= \text{arg}(A_1 - A_2)$ . Perform ing integration, one obtains,

$$P^{(s;osc)}(E) / Ce^{F_0=g^2} cos S=g^2 + F_0^0 S^{0^2}=2 exp - \frac{2}{4}(F_0^0 S^0)$$
:

Taking into account that  $F_0^0 = F_1^0$  we see that the interference term is suppressed by the additional factor  $\exp f^{-2}$  S  $^{\circ 2}=4g$  with respect to the dominant contribution (46). Below we x=1. We observed that the interference patterns get multiplied by  $10^{-3}$  in this case; the latter number is accepted as the precision of the smoothening. The graph of the function  $P^{(s)}$  (E) is shown in Fig. 14, dashed line.

Our nal remark concerns the physical meaning of the smoothening procedure. In a realistic experiment one cannot x the energy E of the incoming particles exactly; rather, one works with some sharply peaked energy distribution D of a width E. Formula (45) represents averaging over such distribution.

Now, we are ready to consider the  $\lim it g^2$ ! 0. Our aim is to check the following asymptotic formula, cf. Eq. (1),

$$P^{(s)}(E;N)! g A(E;N)e^{F(E;N)=g^2}$$
 as  $g^2! 0:$  (48)

We compute the value of the quantity  $g^2 \log P^{(s)}$  at several  $g^2 = 1$ , keeping E and N xed, and the graph with the expression

$$g^2 \log P^{(s)} = F$$
  $g^2 \log g$   $g^2 \log A$ : (49)

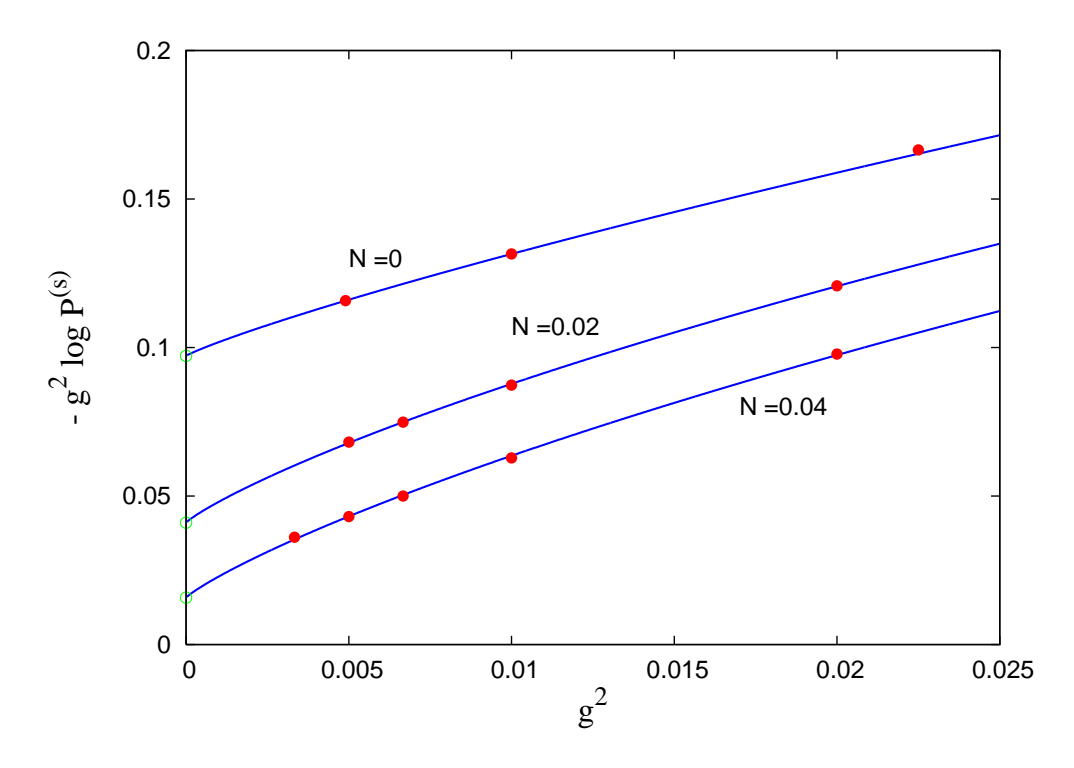


Figure 15: The quantity  $g^2 \log P^{(s)}$  viewed as a function of  $g^2$  at xed N and E = 0.5.

It is in portant to point out that we do not consider as a free param eter of the t. Rather, we use the following result of Ref. [29]: for the sphaleron (mediated processes, such as ours, = 1 at N = 0 (vacuum initial state), and = 2 at N  $\leftarrow$  0. Som e of the num erical results (points) together with their ts by the formula (49) (lines) are shown in Fig. 15. The graphs are drawn for three di erent values of N and E = 0.5. Apparently, our data are well approxim ated by the asymptotic (49). To get the value of the suppression exponent F, one extrapolates the curves in Fig. 15 to the point  $g^2 = 0$ , where the quantum mechanical results should coincide with the semiclassical ones. The error of the extrapolation arises m ainly from the disregarded terms proportional to the higher powers of  $q^2$ . One reduces such errors by computing the rejection probability at the smallest possible q2. In practice we used two values of the sem iclassical parameter in each  $t_r$ , namely, q = 0.1; 0.07 at N = 0, and g = 0.1; 0.08 at N = 0.02; 0.04. The extrapolation error is determined by pouring som e  $10^2$  at smallE to F additional points into the t; it varies from F  $10^4$  at E 10 4 of higher order terms of the semiclassical expansion m atches with the estimate  $0 (q^4)$ which are neglected in Eq. (49).

 $<sup>^{20}</sup>$ For the sake of argument we, again, disregard the boundary terms in the suppression exponent, c.f. Eqs. (24).

Our nalresults for the suppression exponent F (E;N) extracted from the numerical solution of the Schrdinger equation are presented in Fig. 13 (points with error bars standing for the accuracy of the extrapolation). The quantum mechanical results are in very good agreement with the semiclassical ones (lines). This justiles the semiclassical approach presented in this paper.

## 6 Summary and discussion

In this paper we tested the sem iclassical method of complex trajectories in the regime of chaotic dynam ical tunneling. We studied a particular example, over-barrier rejection in the two-dimensional waveguide model (2). The initial state of the process was fixed by the total energy E and occupation number N of the transverse oscillatory motion. We calculated the suppression exponent of the process both sem iclassically and by solving exactly the full Schrodinger equation. The two approaches show very good agreement.

The tunneling trajectories in our sem iclassical approach are obtained as solutions to the boundary value problem (21). We advocated a particular method for inding these solutions. It consists of two important ingredients:

- (i) determ ination of the solution at some values of the initial (state parameters E , N ;
- (ii) gradual deform ation of the solution to other  ${\tt E}$  ,  ${\tt N}$  .

The deform ation procedure (ii) was developed in Refs. [8, 28]. The advantages of this procedure are the simplicity of numerical implementation and generality. It can be applied e ciently to systems with many degrees of freedom, including non (trivial models of eld theory, see Ref. [9].

On the other hand, a generic approach for performing the step (i) was missing so far. In this paper we proposed the systematic procedure which Ils this gap. The procedure enables one to obtain the complex tunneling trajectories starting from the real classical solutions. It is based on the {regularization method of Refs. 27]. Our procedure appears to be generic. It can be applied to any process which proceeds classically at some values of the initial (state parameters (at large N in our case) and becomes exponentially suppressed at other values.

The process we studied is a particular example of chaotic tunneling. The chaoticity manifests itself in the in nite number of tunneling solutions. Our procedure, which connects the tunneling solutions to the classical ones, turns to be highly e cient in this situation. Namely, it enables one to classify the tunneling trajectories on the basis of the analysis of the classical dynamics. This was demonstrated explicitly in the present paper.

In addition, we proposed a heuristic criterion for sorting out the least suppressed tunneling trajectories basing on the classication of their classical progenitors. Hopefully, this criterion will be useful for the processes in other dynamical systems as well.

A nother interesting feature of our setup is the phenom enon of optim altunneling. Namely, the suppression exponent F considered as a function of energy E at xed N is non-monotonic. It attains the local minimum at E 0.5 which is thus (locally) the optimal energy for tunneling. It is worth stressing that this behavior of the suppression exponent is unrelated to the quantum interference, which was neglected in the semiclassical analysis and eliminated from the exact quantum computations. A nother example of tunneling process with non-monotonic dependence of the suppression exponent on energy is considered in Ref. [30].

Let us mention some open issues. The method of complex trajectories is known to suer, in general, from the diculties related to the Stokes phenomenon [12, 13]. The essence of this phenomenon is that the solutions to the tunneling problem may be unphysical in some regions of the parameter space. A coordingly, their contributions to the tunneling probability should be dropped out. Presently, there are no generic criteria for distinguishing between physical and unphysical solutions. The method we put forward in this paper does not provide such criteria either. Note that we did not see any manifestations of the Stokes phenomenon in the semiclassical calculations reported in this paper. In other cases, however, accounting for this phenomenon may be crucial for understanding the tunneling processes, see e.g. [14, 30].

The approach adopted in this paper was to perform the evaluation of the tunneling probability as the system atic sem iclassical expansion in terms of  $g^2$ . We have calculated the leading term (suppression exponent). It is of interest to develop a method for calculating the sub-leading terms, in particular, the pre-exponential factor A, see Eq. (1). Presumably, this can be done along the lines of Ref. [29]. An important problem which should be solved here is how to cope with the in nite number of tunneling paths, whose suppressions can be arbitrarily close to the limiting value. In particular, one has to understand whether the contributions of all the paths should be summed up or the correct value of the prefactor is determined by a sort of limiting procedure similar to the one we used to obtain the suppression exponent.

A nother question is the following one. While solving the Schrodinger equation we observed that at nite  $g^2$  the dependence of the exact tunneling probability on energy is modulated by oscillations. We conjectured that they result from the quantum interference of dierent tunneling trajectories. In the true semiclassical limit  $g^2$ ! O the above oscillations become in nitely frequent and should be averaged over. In real physical situations

one deals, however, with small but nite values of the sem iclassical parameter  $g^2$ . Thus it is worth understanding whether the interference pattern mentioned above can be reproduced in the sem iclassical approach. Can it be done by sum ming up the contributions of various tunneling trajectories at nite  $g^2$ ? To what accuracy can that be done? We leave these questions for the future work.

A cknow ledgm ents We are indebted to F.L.Bezrukov and V.A.Rubakov for useful discussions and helpful suggestions. This work was supported in part by the RFBR grant 05-02-17363, Grants of the President of Russian Federtion NS-7293 2006 2 (government contract 02.445.11.7370), MK-2563 2006 2 (D.L.), MK-2205 2005 2 (S.S.), the Grants of the Russian Science Support Foundation (D.L. and S.S.), the Fellow ship of the \Dynasty" Foundation (awarded by the Scientic board of ICPFM) (A.P.) and the INTAS grant YS 03-55-2362 (D.L.). D.L. is grateful to the Universite Libre de Bruxelles and to EPFL, Lausanne, for the hospitality during his visits. The numerical calculations were performed on the Computational cluster of the Theoretical division of INR RAS.

### A A method to obtain the unstable solutions

In this Appendix we describe the numerical method used to obtain the limiting tunneling trajectories considered in Sec. 4, namely, the ones ending up at the far sphaleron at late times. The main problem here is the instability of the trajectories in question.

Our main idea is to add the following term to the action functional,

$$S[x]$$
7  $S[x]$  +  $iM$   $(x(t_f) x_f^0)^2$ ; (50)

where x ( $t_f$ ) stands for the nalvalue of the coordinate x, while M>0,  $x_f^0$  are real parameters. For a given trajectory the term (50) leads to additional contribution to the suppression exponent,

$$F = 2M (x (t_f) x_f^0)^2$$
: (51)

The introduction of the above term induces the following modication of the boundary conditions (21c),

$$Im x(t_f) = 0; (52a)$$

$$\operatorname{Im} \, \underline{\mathbf{x}}(\mathsf{t}_{\mathrm{f}}) = 2 \, \operatorname{M} \, \left( \mathbf{x} \left( \mathsf{t}_{\mathrm{f}} \right) \quad \mathsf{x}_{\mathrm{f}}^{0} \right) \, \mathbf{:} \tag{52b}$$

This can be shown using the system atic approach of Refs. [27, 29, 30]. At large positive M the term (51) xes the value of the nalx-coordinate of the solutions to be close to  $x_f^0$ . For our purposes we choose  $x_f^0$  to be in the vicinity of the far sphaleron,  $x_f^0 = 1$ . Solutions which approach the far sphaleron at late times are obtained in the following way. One note a solution to the original equations of motion which spends nite time on the far sphaleron, and cuts it at the moment  $t = t_f$  when it is still at x = 1. Using this trajectory as the zeroth (order approximation, one applies the Newton (Raphson algorithm and obtains the solution satisfying the boundary conditions (52). The latter solution is defined inside the interval  $t \ge [t_i; t_f]$ . The next step is to continue the solution to a larger time interval by gradually increasing the value of  $t_f$  and deforming the tunneling solution. As a result, one obtains the solution living at the far sphaleron for an arbitrarily long time.

The solution obtained in this way does not, strictly speaking, satisfy the boundary conditions (21c) of the tunneling problem . In order to restore the original boundary conditions (21c) one should, in principle, investigate the dependence  $x_f(x_f^0)$  and not the value of  $x_f^0$  which solves the equations  $x_f(x_f^0) = x_f^0$ . However, it is not necessary in our case: at late times the limiting solution is almost real, so one obtains Im  $x_f^0$  0 automatically.

## B Num erical solution of the Schrodinger equation

Here we present the numerical formulation of the problem (36), (39), (40). First of all, the range of the translatory coordinate should be bounded, L X L, as well as the oscillator excitation number,  $n < N_y$ . Besides, we introduce the uniform lattice with spacing

$$X_k = L + (k + 1)$$
;  $k = 1; ::: ; N_x + 1$ ;

where  $N_x = 2 + 2L = .$  The Taylor series expansion gives,

$$\frac{1}{2} \begin{bmatrix} k+1 & 2k+k \end{bmatrix} = k + \frac{2}{12} + \frac{(IV)}{k} + O(k^4) :$$
 (53)

By  $_{k}^{0}$  and  $_{k}^{(IV)}$  we denote the second and fourth derivatives of at  $X = X_{k}$ . Note that the index n is suppressed: hereafter we use the matrix notations. From Eq. (36)  $_{k}^{0} = A_{k}$  if or the fourth derivative one writes,

$$_{k}^{(IV)} = \frac{1}{2} \quad _{k+1}^{0} \quad 2_{k}^{0} + \quad _{k-1}^{0} + O(^{2}) = \frac{1}{2} \left[ A_{k+1-k+1} \quad 2A_{k-k} + A_{k-1-k-1} \right] + O(^{2}) :$$

Substituting the above expressions into Eq. (53), one gets the forth {order N um erov {C ow ling approximation for Eq. (36),

$$1 \quad \frac{2}{12} A_{k+1} \quad _{k+1} \quad 2 + \frac{5}{6} A_k \quad _{k} + \quad 1 \quad \frac{2}{12} A_{k-1} \quad _{k-1} = 0; \quad k = 0; :::; N_x :$$
(54)

It is worth noting that Eq. (54) supports the discrete probability current, which is conserved exactly,

$$J^{(d)} = \frac{1}{2} \text{Im} \quad {}_{k}^{+} \quad 1 \quad \frac{2}{12} A_{k} \quad 1 \quad \frac{2}{12} A_{k+1} \quad {}_{k+1} : \tag{55}$$

This conservation law was used to estimate the round (o errors.

The boundary conditions (39), (40) are in posed at the very last and rst sites,  $k = N_x + 1$  and 1 respectively. One notes that the asymptotic formula  $\beta$ 7) holds in the discrete case as well, provided the continuum dispersion relation (38) is replaced with the discrete one<sup>21</sup>,

$$P_n ! P_n^{(d)} = \frac{2}{a} \arcsin \frac{P_n}{2} \frac{P_n}{1 + P_n^2} :$$

Consequently, one rewrites Eqs. (39), (40) as

These relations together with Eq. (54) form a system of N $_{\rm y}$  (N $_{\rm x}$  + 3) linear equations for the same number of unknowns  $_{\rm n;k}$ . A fter solving them, one calculates the rejection probability by making use of the discrete current,

$$P = \frac{jJ^{(d;out)}j}{jJ^{(d;in)}j};$$

where J  $^{(d;in)}$  and J  $^{(d;out)}$  are the incom ing and outgoing currents at  $k=N_x+1$ ,

$$J^{(d;out)} = \frac{1}{n} \frac{X}{\sin(P_n^{(d)})jr_n^{+\frac{2}{2}}}; \qquad J^{(d;in)} = \frac{1}{1} \frac{\sin(P_N^{(d)})}{1 \frac{1}{3}\sin^2\frac{P_N^{(d)}}{2}};$$

while the re-ection amplitudes  $\boldsymbol{r}_n^{\scriptscriptstyle +}$  are extracted from the wave function,

$$r_n^+ = \frac{n N_x + 1}{1} \frac{e^{iP_n^{(d)}}}{e^{2iP_n^{(d)}}} e^{iN_x} e^{iP_n^{(d)}L} :$$

 $<sup>^{21}</sup>$ For n > E 1=2 one has  $P_n^{(d)} = \frac{2i}{2} \operatorname{arcsh} \frac{p}{2} \frac{p_n j}{1 p_n j^2}$ 

We will see shortly that the nite dierence approximation works well only if the numbers of the lattice points and oscillator levels are large. Typically,  $N_x$  10000,  $N_y$  500, and the system (56), (54) contains  $N_y$  ( $N_x + 3$ ) 5 10 equations. Such an enormous system of equations cannot be solved with the general algorithms of linear algebra. So, we took advantage of the special form of Eqs. (54). Namely, the k-th matrix equation relates the vector k to the unknowns at the adjacent sites k and k and k only; by performing numerically the matrix inversion it can be recast in the form

$$_{k} = L_{k} _{k} _{1} + R_{k} _{k+1}$$
;

where  $L_k$  an  $R_k$  are the  $N_y$   $N_y$  m atrices. One substitutes the above formula into the other equations of the system (54), thus excluding k, as well as the k {th matrix equation. Performing this operation repeatedly, one ends up with a few matrix equations, which can be solved in a straightforward manner by the LU decomposition method. It is worth pointing out that the variables k and k which are not neighbors to each other, can be excluded in parallel, so that the above algorithm is suitable for the multiprocessor machines or computational clusters. The reader interested in the details of the algorithm should address Refs. [28], [28], or our Fortran 90 code [33], which hopefully can be executed on other machines.

Before proceeding to the actual calculations, one makes sure that the parameters of the lattice are chosen properly, so that the truncation and discretization errors are kept under control. Our purpose is to get the quantum mechanical results in the semiclassical region  $g^2$ ! O. Therefore, it is convenient to account explicitly for the dependence of the lattice parameters on g. The truncation L of the translatory coordinate is xed by the condition that the interaction represented by the function a(X) is small enough at X = L. Taking into account the scaling (35) of a(X) with g, one obtains the formula

$$L = \widetilde{L} = q$$
;

where  $\Gamma$  is xed and large. In the practical calculations we used the value  $\Gamma = 12$ , which is large enough as a ( $\Gamma$ ) 10  $^{31}$ : at g > 0.07 this number is smaller than the absolute values of the rejection amplitudes, the latter exceeding 10  $^{8}$ . We have chosen the truncation of the oscillator levels in accordance with the condition that the occupation number of the last mode is negligible,

this inequality was satis ed with N  $_{\rm y}$  typically ranging in between 200 and 500. The last parameter, the lattice spacing , should be several times smaller than the minimal D e

Broglie wavelength; we have found that the formula

$$= 0:3 \quad \min_{n} \frac{1}{P_n}$$

works well enough producing relative errors of order 10 4.

The fact that the discretization corresponds to the relative rather than absolute errors can be understood as follows. The equations (54) and (56) m ay be regarded as the ones describing re ection of a quantum particle in a kind of crystal<sup>22</sup>. The probability of this process is exponentially small due to the same dynamical reasons as in the continuum case. One concludes that the nite value of gives rise to corrections to the suppression exponent, rather than to the rejection probability itself, i.e. it produces relative discretization errors. We have checked the above physical considerations by performing calculations on the lattices with different cuto s and lattice spacings. The overall conclusion is that, indeed, the discretization exponents are always negligible. We kept the round (or errors under control by exploiting the current conservation law (55), which was checked to hold with precision better than 10. 12.

## References

- [1] A.M. Perelom ov, V.S. Popov and M.V. Terent'ev, ZHETF 51, 309 (1966). V.S. Popov, V. Kuznetsov and A.M. Perelom ov, ZHETF 53, 331 (1967).
- [2] W .H.Miller, Adv.Chem.Phys.25, 69 (1974).
- [3] I.Y.Kobzarev, L.B.Okun and M.B.Voloshin, Sov.J.Nucl.Phys. 20, 644 (1975) [Yad.Fiz. 20, 1229 (1974)].
  - S.R.Coleman, Phys. Rev. D 15, 2929 (1977) [Erratum ibid. D 16, 1248 (1977)].
- [4] M.Davis and E.Heller, J.Chem Phys. 75, 246 (1981).
- [5] M.W ilkinson, Physica 21D, 341 (1986).
  - S.Takada and H.Nakamura, J.Chem. Phys. 100, 98 (1994).
  - S. Takada, P. Walker and M. Wilkinson, Phys. Rev. D 52, 3546 (1995).
  - S. Takada, J. Chem. Phys. 104, 3742 (1996).

<sup>&</sup>lt;sup>22</sup>This analogy becomes apparent after the substitution  $_k = 1 - \frac{^2}{12} A_k$  which brings Eq. (54) into the form H <sup>(d)</sup> = 0, where is the column composed of  $_k$ , and H <sup>(d)</sup> is a Herm itean linear operator.

- [6] T.Banks, C.M. Bender and T.T.Wu, Phys. Rev. D 8, 3346 (1973).
  T.Banks and C.M. Bender, Phys. Rev. D 8, 3366 (1973).
- [7] V.A.Rubakov, D.T.Son and P.G.Tinyakov, Phys. Lett. B 287, 342 (1992).
- [8] A. N. Kuznetsov and P. G. Tinyakov, Phys. Rev. D 56, 1156 (1997) [arX iv:hep-ph/9703256].
- [9] F. Beznukov, D. Levkov, C. Rebbi, V. A. Rubakov and P. Tinyakov, Phys. Rev. D 68, 036005 (2003) [arX iv hep-ph/0304180]; Phys. Lett. B 574, 75 (2003) [arX iv hep-ph/0305300].
- [10] D. G. Levkov and S. M. Sibiryakov, Phys. Rev. D 71, 025001 (2005) [arX iv hep-th/0410198]; JETP Lett. 81, 53 (2005) [Pisma Zh. Eksp. Teor. Fiz. 81, 60 (2005)] [arX iv hep-th/0412253].
- [11] I.A eck, Nucl. Phys. B 191, 429 (1981).
- [12] M.V.Berry and K.E.Mount, Rep Prog Phys. 35, 315 (1972).
- [13] S.Adachi, Ann Phys. 195, 45 (1986).
- [14] A. Shudo, K. S. Ikeda, PhysRev Lett. 76, 4151 (1996).
- [15] O.Bohigas, S. Tom sovic and D. Ullmo, Phys. Rep. 223, 43 (1993).
- [16] E.Doron and S.D. Frischat, Phys. Rev. Lett. 75, 3661 (1995);S.D. Frischat and E.Doron, Phys. Rev. E 57, 1421 (1998).
- [17] A.Mouchet, C.Miniatura, R.Kaiser, B.Gremaud, D.Delande, Phys. Rev. E 64,016221 (2001).
- [18] A. Shudo, K. S. Ikeda, Phys. Rev. Lett. 74, 682 (1995); Physica D 115, 234 (1998).
- [19] A. Shudo, Y. Ishii and K.S. Ikeda, J. Phys. A 35, L225 (2002).
- [20] V. I. Amold, A. Avez, Ergodic Problems of Classical Mechanics," Benjamin, New York, 1968.
- [21] V.I.Zakharov, Nucl. Phys. B 353, 683 (1991); Phys. Rev. Lett. 67, 3650 (1991).
  G. Veneziano, Mod. Phys. Lett. A 7, 1661 (1992).

- [22] M.Maggiore and M.A.Shifman, Phys. Rev. D 46, 3550 (1992).
- [23] M.B. Voloshin, Phys. Rev. D 49, 2014 (1994).
- [24] V.A. Rubakov and D.T. Son, Nucl. Phys. B 424, 55 (1994) [arX iv hep-ph/9401257].
- [25] C.S.Drew, S.C.Creagh and R.H.Tew, Phys. Rev. A 72, 062501 (2005).
- [26] F.R.K linkham er and N.S.M anton, Phys. Rev. D 30, 2212 (1984).
- [27] F. Beznukov and D. Levkov, arX iv quant-ph/0301022; J. Exp. Theor. Phys. 98, 820 (2004) [Zh. Eksp. Teor. Fiz. 125, 938 (2004)] [arX iv quant-ph/0312144].
- [28] G.F.Bonini, A.G.Cohen, C.Rebbi and V.A.Rubakov, Phys.Rev.D 60, 076004 (1999) [arX iv:hep-ph/9901226]; arX iv:quant-ph/9901062.
- [29] D.G. Levkov, A.G. Panin and S.M. Sibiryakov, \Tunneling via unstable sem iclassical solutions: a system atic approach.", in preparation
- [30] D.G. Levkov, A.G. Panin and S.M. Sibiryakov, \On the over-barrier re ection in quantum mechanics with many degrees of freedom," in preparation
- [31] W H. Press, S.A. Teukolsky, W. T. Vetterling, B.P. Flannery, \Numerical recipes in C: the art of scientic computing", Cambridge University Press, 1992.
- [32] D. Levkov, C. Rebbi and V. A. Rubakov, Phys. Rev. D 66, 083516 (2002) [arX iv gr-qc/0206028].
- [33] http://solver.inr.ac.ru